SmartMat

WILEY | 天津大学 Tianjin University

REVIEW OPEN ACCESS

Recent Advances in Metal-Organic Framework-Integrated Nanocomposite Hydrogels for Sensors and Sensing Systems

Md Sazzadur Rahman | Emna Helal | Nicole R. Demarquette

Department of Mechanical Engineering, Ecole de Technologie Superieure, Montreal, Canada

Correspondence: Nicole R. Demarquette (nicoler.demarquette@etsmtl.ca)

Received: 17 September 2025 | **Revised:** 29 October 2025 | **Accepted:** 18 November 2025

Funding: Tier 1 Canada Research Chair, Grant/Award Number: CRC-2021-00489

Keywords: hydrogel | metal-organic frameworks | polymer composites | sensing platforms | sensors | smart materials

ABSTRACT

Metal-organic frameworks (MOFs) are versatile crystalline porous materials with large surface areas, tunable pore architectures, and modular chemical functionalities, enabling diverse applications in materials science and engineering. Hydrogels, with their softness, high water content, biocompatibility, and responsiveness to external stimuli, have been widely explored as smart platforms for flexible electronics and sensing technologies. Integrating MOFs into hydrogel networks synergistically combines the advantages of both material classes, yielding multifunctional composites with enhanced structural and functional properties. MOF–hydrogel composites overcome the limitations of each component, offering improved mechanical robustness, environmental stability, and dynamic responsiveness, making them highly promising for next-generation sensing systems. This review provides a comprehensive overview of recent advances in the synthesis, structural design, and characterization of MOF–hydrogel composites, with a focus on their applications in optical, electrochemical, and electromechanical sensing. Their use across healthcare diagnostics, environmental monitoring, food safety, public health, and flexible electronics is discussed. We highlight how MOF–hydrogel integration influences key sensing metrics such as selectivity, sensitivity, adaptability, detection limits, long-term stability, and dynamic working range. In summary, this review highlights the crucial role of MOF–hydrogel composites in advancing high-performance sensing technologies, outlining key challenges and future directions to inform ongoing research in this field.

1 | Introduction

Over the past few decades, metal-organic frameworks (MOFs) have emerged as one of the most rapidly advancing classes of crystalline porous materials, attracting considerable attention across chemistry, materials science, and engineering disciplines [1, 2]. Their exceptional chemical versatility, optical and physical tunability, high surface areas, well-defined pore structures, and structural diversity have positioned MOFs as unique and highly functional nanomaterials. A key advantage of MOFs lies in their modular synthesis, which allows for the precise tuning of their properties by strategic selection of metal nodes and organic linkers. As a result, more than 95,000 distinct MOF structures have been reported to date, encompassing a wide range of topologies, porosities, and functionalities [3–5].

As illustrated in Figure 1A, the unique properties of MOFs offer unparalleled diversity, enabling their customization for specific applications. This versatility has led to their extensive use in gas separation and storage [6], catalysis [7–9], membrane technologies [10], energy storage and conversion devices (e.g., batteries and supercapacitors) [11–18], sensing platforms [19, 20], drug

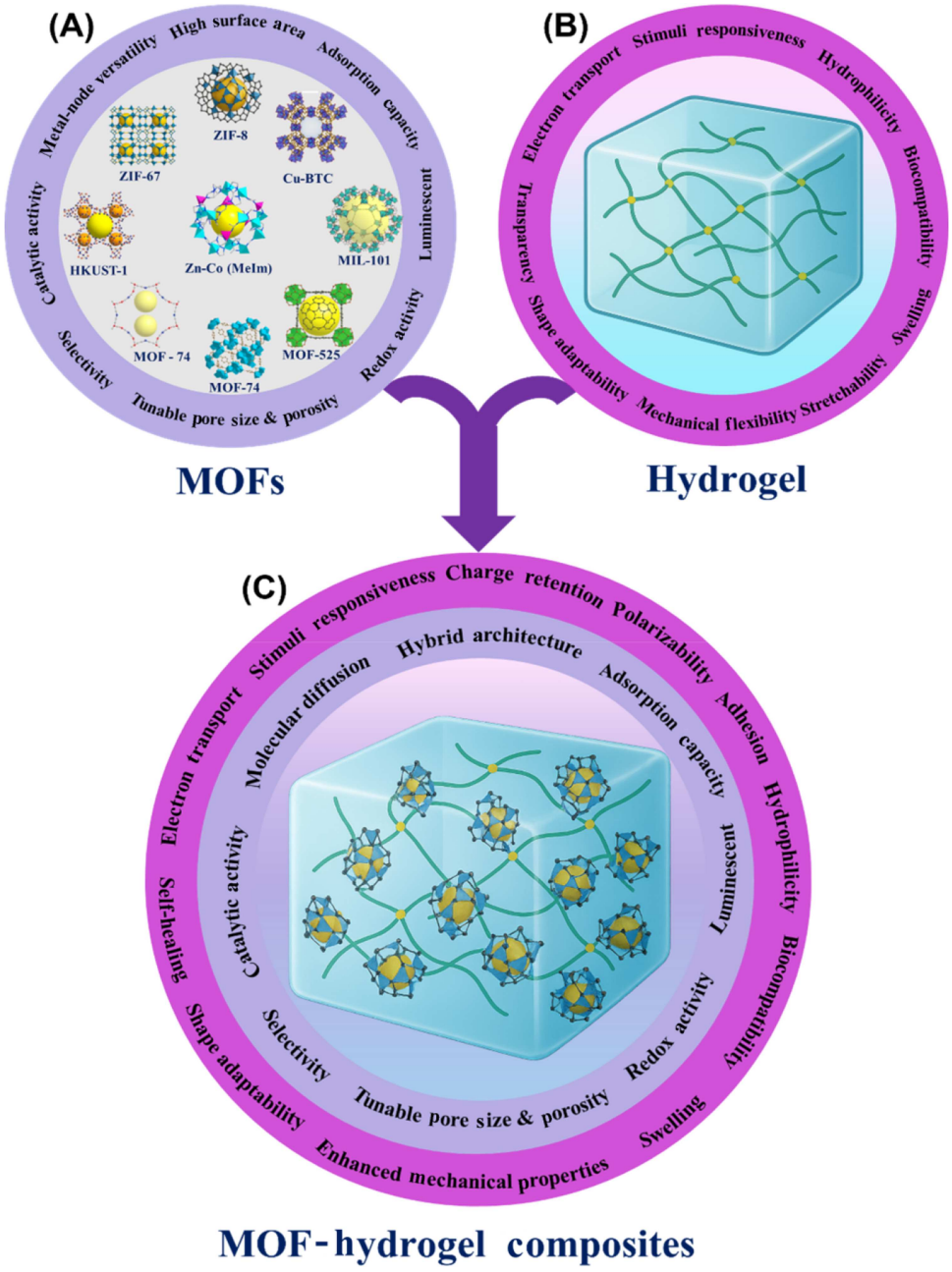

FIGURE 1 | (A) Schematic representation of MOF nanoparticles highlighting their significant structural and functional advantages for sensing applications. (B) Schematic representation of the unique properties of hydrogels. (C) Illustration of a MOF–hydrogel hybrid architecture that combines the complementary properties of both materials in a single platform, thereby overcoming the individual limitations of MOFs and hydrogels for enhanced sensing applications.

delivery [21–23], and environmental remediation [24, 25]. The continuous innovation in MOF design and functionalization strategies underscores their immense potential to address pressing challenges in energy, environmental sustainability, and advanced material development. Furthermore, owing to their tunable multifunctionality, nanoscale dimensions, and microporous structures, MOFs have garnered increasing interest as functional reinforcing additives for chemically inert composites.

Concomitantly, hydrogels are recognized as one of the most innovative classes of soft materials due to their inherent flexibility, stretchability, biocompatibility, mechanical recoverability, stimuli-responsiveness, hydrophilicity, optical transparency, high water content, and tissue-like mechanical properties, as highlighted in Figure 1B [26–29]. These unique features closely mimic the physical characteristics of natural extracellular matrices, making hydrogels highly attractive for a wide range of applications. As a result, hydrogels have been extensively explored in diverse fields such as flexible and wearable sensors and electronics [30–34], soft robotics [35, 36], energy storage systems [37], tissue engineering scaffolds [38], bioengineering platforms [39, 40], regenerative medicine therapies, wound healing, drug delivery systems [41], and environmental remediation technologies [42]. Their intrinsic ability to respond to external stimuli, combined with their biocompatibility and tunable physical properties, has further expanded their utility across interdisciplinary research areas.

Nevertheless, despite their remarkable advantages, conventional hydrogels often suffer from limitations such as relatively low mechanical strength, limited electrical conductivity, and restricted functional tunability. To overcome these challenges and further enhance hydrogel performance, significant research efforts have focused on integrating functional nanomaterials into hydrogel matrices. Among these, carbon-based materials have been widely utilized for nanocomposite hydrogel sensing applications due to their excellent electrical conductivity [43–45]. Although numerous studies have demonstrated their advantages, their applications have largely remained limited to electromechanical or physical sensing systems, rather than encompassing a broader range of sensing modalities [46, 47]. However, carbon-based nanomaterials also exhibit several drawbacks, including high production costs, limited chemical tunability, relatively low surface area, restricted functionality, challenges in surface functionalization, and an inherently hydrophobic nature. In contrast, MOFs can overcome these drawbacks owing to their tunable size, surface chemistry, metal nodes, and structural diversity, providing enhanced design flexibility and functionality for next-generation multifunctional sensing systems. As a result, MOF-based nanocomposite hydrogels have attracted particular attention, as they provide an excellent platform for leveraging the unique properties of MOFs to enhance overall material performance. The incorporation of MOFs within hydrogel networks has enabled the development of systems with improved mechanical robustness, enhanced responsiveness, and multifunctionality, thereby driving notable progress in the fields of polymer science and composite materials engineering. As shown in Figure 1C, given the diverse and complementary properties of MOFs and hydrogels, the incorporation of MOFs as functional reinforcing fillers into hydrogel matrices has opened new avenues for the development of next-generation optical, electrochemical, and electromechanical sensing platforms, particularly for applications requiring flexible, wearable, and biologically compatible devices.

To date, several review papers on MOF–hydrogel composites have been published, primarily focusing on state-of-the-art fabrication strategies and their functional advancements. For example, Wang et al. [48] reviewed recent progress in MOF-based hydrogels and aerogels, emphasizing synthesis strategies, structural classifications, and multifunctional properties. While their work highlighted applications in wound healing, water purification, catalysis, and energy-related systems, it did not comprehensively address MOF-based sensors and their emerging applications in sensing technologies. Similarly, Sun et al. [49] provided a comprehensive overview of engineering strategies for the preparation of MOF-based hydrogels, categorizing them according to different MOF types. Their review further discussed the broad applications of these materials in environmental, energy, and biomedical fields, while also offering perspectives on future directions in MOF–hydrogel research. Focusing more specifically on biomedical applications, Lim et al. [50] reviewed biomedically relevant MOF–hydrogel composites, emphasizing synthesis strategies, structural design considerations, and potential applications in areas such as drug delivery, tissue engineering, and biosensing. They also discussed challenges associated with integrating MOFs into hydrogels while maintaining biocompatibility and functional performance. In addition, Zhuang et al. [51] reviewed strategies for the conversion between MOFs and gel materials, focusing on design principles and synthetic methodologies for the sensing field. However, their work primarily concentrated on MOF-derived organic gels and metal-organic gels, rather than on hydrogel-based systems. Furthermore, several studies have focused exclusively on MOF-based sensors, with limited attention given to composites in which MOFs are embedded within or structurally reinforced by hydrogels or other supporting matrices. In the context of wearable technologies, Meskher et al. [52] presented a mini-review on MOF-based wearable sensors, discussing current challenges and opportunities for advancing MOFs in flexible and wearable sensing platforms. They highlighted critical issues such as material integration, mechanical stability, and real-world applicability, while also proposing future directions for research in this emerging field. Broadening the scope to electronic integration, Stassen et al. [53] provided an updated roadmap for the application of MOFs in electronic devices and chemical sensors, addressing key challenges related to processing, interfacing, and scaling MOFs for practical device applications. Their review also outlined strategic approaches to advance MOF-based electronics and sensing technologies. Moreover, other reviews have comprehensively covered the use of MOF-based sensors for detecting exogenous contaminants in food, portable fluorescence sensing and visual detection applications, agricultural monitoring of metal ions, gas and volatile compound detection, environmental contaminant sensing, and electrochemical sensing platforms [54–59]. Despite these valuable contributions, reviews specifically addressing MOF–hydrogel composite-based sensors remain lacking, as most existing studies have primarily concentrated on MOFs without emphasizing hydrogel integration for sensing applications. Notably, where sensors were discussed, the focus was often limited to specific sensing platforms rather than providing a detailed and multidisciplinary overview of broader sensing fields and applications.

Considering the unique advantages offered by both hydrogels and MOFs, this review comprehensively and systematically summarizes the state-of-the-art developments and recent progress of MOF–hydrogel composites as a promising class of advanced high-performance materials for sensing applications. These hybrid systems combine the excellent flexibility, biocompatibility, and stimulus-responsiveness of hydrogels with the high porosity, tuneable chemistry, and structural versatility of MOFs, resulting in multifunctional composites uniquely suited for sensing technologies. Particular emphasis is placed on their applications across physical, chemical, electrochemical, and optical sensing domains. Using this overview as a foundation, we further highlight key challenges, emerging opportunities, and future research directions to advance the rational design, fabrication, and functional integration of MOF–hydrogel composite-based sensors. Following a detailed summary of the strategies employed for the synthesis and characterization of MOF–hydrogel composites, this review discusses representative examples demonstrating their use in diverse sensing platforms, including physical sensors, chemical analyte detection, biosensing, and environmental monitoring. Wherever possible, we endeavor to elucidate how the integration of MOFs into hydrogel matrices confers unique enhancements, such as improved selectivity, sensitivity, multi-stimuli responsiveness, and environmental stability. In addition, we

explore how recent advancements in MOF chemistry, such as stimulus-triggered structural transformations or optical properties, can be harnessed to expand the capabilities of MOF–hydrogel-based sensors. Finally, we conclude with our perspectives on the critical challenges that must be addressed and future opportunities that must be leveraged to fully realize the potential of MOF–hydrogel composites in next-generation sensing technologies.

2 | Fabrication Strategies for MOF-Integrated Hydrogels for Sensing Applications

The successful development of MOF–hydrogel composites for sensing applications relies heavily on the selection of fabrication strategies that enable effective integration of MOFs into hydrogel matrices without compromising the intrinsic advantages of either component. Given the distinct physicochemical properties of MOFs, such as high surface area, porosity, and chemical tunability, and the structural softness and aqueous compatibility of hydrogels, designing composite systems requires careful consideration of material compatibility, stability, loading efficiency, and network homogeneity. In sensing platforms, particularly those intended for wearable, stretchable, or biocompatible environments, the method of MOF incorporation can significantly influence the mechanical integrity, signal responsiveness, and overall performance of the composite sensor. In this section, we focus specifically on the fabrication approaches used to develop MOF–hydrogel composites, rather than on the synthesis of standalone MOFs, which have been thoroughly reviewed elsewhere [60–67]. Instead, we emphasize the various strategies by which MOFs are integrated, embedded, or distributed within hydrogel networks, and how these composite systems are fabricated and tailored to achieve optimal performance in sensing applications. MOF nanoparticles can either be pre-synthesized and incorporated into hydrogels or synthesized in situ within the hydrogel matrix. They can also be directly fabricated during additive manufacturing. The three approaches for obtaining MOF–hydrogel composites are reviewed below.

2.1 | Physical Embedding of Pre-Synthesized MOF Nanoparticles Into Hydrogel Matrices

Incorporating pre-synthesized MOF particles into hydrogel networks is commonly achieved through physical embedding strategies. These approaches differ based on the sequence of MOF and hydrogel formation, the type of interactions between the two components, and the processing methods employed. Understanding these distinctions is essential for engineering MOF–hydrogel systems with enhanced sensing performance and application-specific functionality. A widely adopted physical embedding method involves dispersing pre-synthesized MOF powders into a pre-gel monomer or polymer solution, a process referred to as direct mixing. As the hydrogel network forms through gelation, the MOF fillers become uniformly entrapped within the matrix. This technique is valued for its simplicity, versatility, and ability to preserve the structural and chemical integrity of MOFs without requiring additional modification [50, 68, 69]. In this review, we categorize fabrication strategies based on the physical embedding of MOFs and the type of hydrogel network formation. Hydrogel matrices can be established either through non-covalent interactions, such as physical or ionic crosslinking, or through covalent approaches like free-radical polymerization, which typically require thermal or photoinitiators. The following sections describe these approaches in detail.

2.1.1 | *Physical Crosslinking With Embedded MOFs*

To fabricate MOF–hydrogel composites for sensing applications, physical crosslinking methods are commonly employed. These approaches allow pre-synthesized MOF nanoparticles to be effectively incorporated into hydrogel networks, with the choice of polymer influencing the resulting stability and performance. Physically crosslinked hydrogels are typically formed through intermolecular reversible interactions, including hydrogen bonding, polymer chain entanglements, crystallization, ionic interactions, and hydrophobic associations [70–72]. These interactions result in stable, yet reversible, three-dimensional (3D) polymer networks that can effectively entrap MOF particles without the need for chemical crosslinking agents. Among the various polymer matrices explored, polyvinyl alcohol (PVA), agarose, carrageenan, alginate, and chitosan (CS) have been the most commonly utilized due to their excellent biocompatibility, flexibility, and ability to form robust physically crosslinked networks [73–81]. The combination of these polymers with MOF nanoparticles has shown considerable promise in enhancing the structural integrity and functional performance of hydrogel-based sensing platforms. For example, Mukundan et al. [73] demonstrated the fabrication of a wearable sweat sensor based on a novel bimetallic iron (Fe) and cobalt (Co) MOF incorporated into a PVA–CS hydrogel matrix. The Fe/Co-MOF was first synthesized via a solvothermal method, and the resulting dried MOF powder was subsequently dispersed into the PVA–CS solution. The hydrogel was then physically crosslinked to entrap the MOF particles within the network, followed by lyophilization for 24 h to obtain the final MOF–hydrogel composite sensor. A schematic representation of the fabrication process utilizing physical crosslinking with embedded MOFs is shown in Figure 2A [73]. In addition to this example, several studies have reported the use of physical crosslinking with embedded MOFs to incorporate pre-synthesized MOF nanoparticles into hydrogel matrices for diverse sensing and sensory system applications [80–88]. A comprehensive summary of these reports, along with other fabrication methods, is provided in Table 1 [73, 74, 89–117].

2.1.2 | *Ionic Crosslinking With Embedded MOFs*

Ionic crosslinking, a form of physical crosslinking, has also been employed in the fabrication of MOF–hydrogels for sensor development. This approach has been primarily applied to hydrogels based on naturally derived polysaccharides, such as alginate, which serve as the hydrogel matrix. Ionic crosslinking involves the formation of a 3D polymer network through electrostatic interactions between negatively charged functional groups on the polymer chains and multivalent cations, such as calcium (Ca^{2+}), aluminum (Al^{3+}), and barium (Ba^{2+}), which act as crosslinking agents [121, 122]. For example, Jiang et al. [82] employed ionic crosslinking to fabricate a MOF-embedded, hydrogel-based ratiometric fluorescence sensor. Pre-synthesized

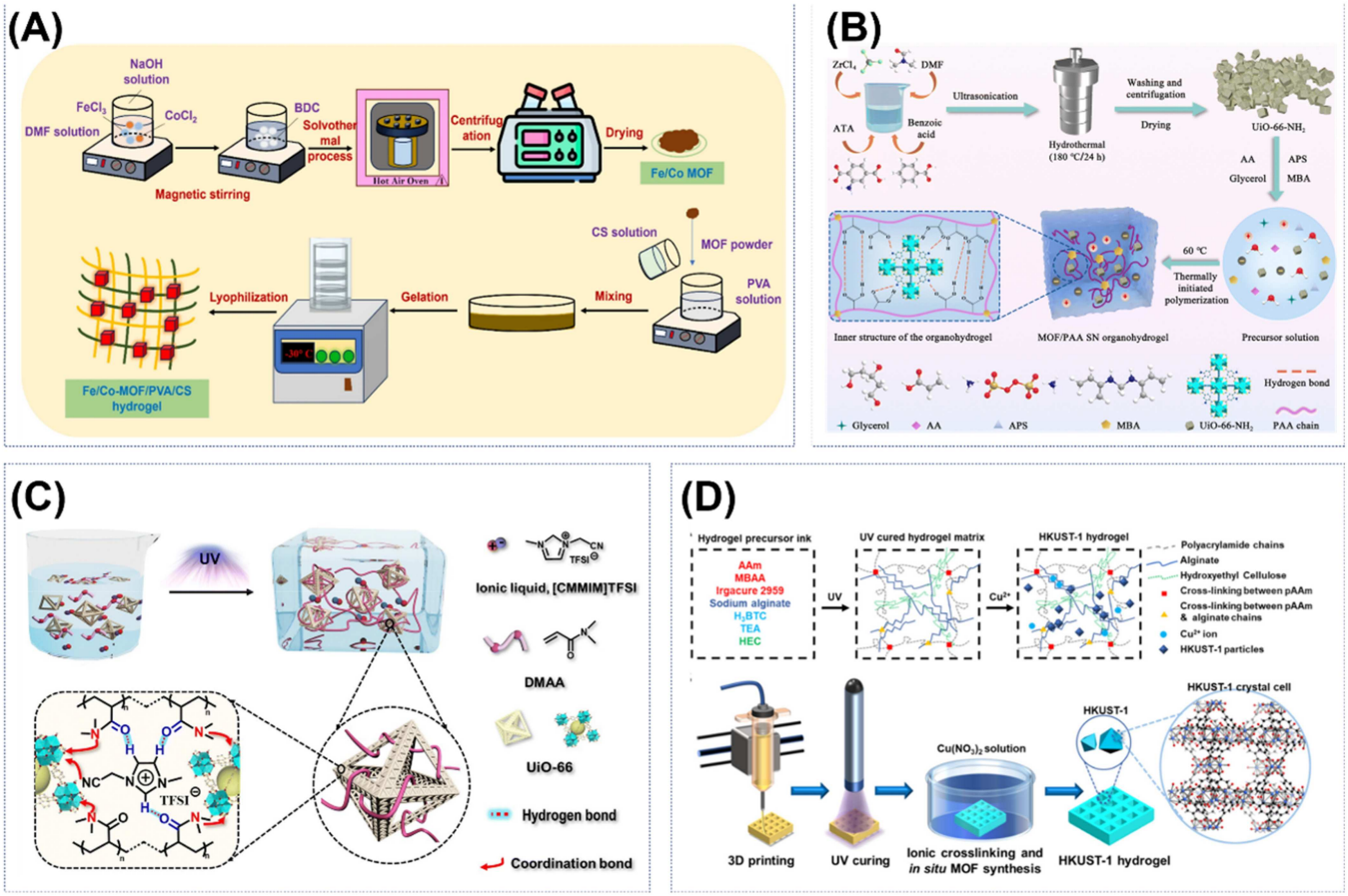

FIGURE 2 | Fabrication strategies of MOF–hydrogel composites used for diverse sensing applications. (A) Schematic of Fe/Co-MOF double-network hydrogel preparation using physical embedding followed by lyophilization. Reproduced with permission: Copyright 2024, Springer Nature [73]. (B) Schematic diagram of the preparation of UiO-66-NH_2 integrated PAM hydrogel via thermally initiated free-radical polymerization. Reproduced with permission: Copyright 2025, Royal Society of Chemistry [118]. (C) Schematic illustration of the fabrication of an ionic DMAA hydrogel incorporating UiO-66 MOF via UV-initiated free-radical polymerization. Reproduced with permission: Copyright 2019, Royal Society of Chemistry [119]. (D) Schematic illustration of the 3D printing process for MOF–hydrogel fabrication, including printing, UV curing, and ionic crosslinking of a PAM–alginate hydrogel matrix incorporated with HKUST-1. Reproduced with permission: Copyright 2020, American Chemical Society [120].

UiO-66 MOF particles were uniformly dispersed in a sodium alginate (SA) pre-gel solution, followed by the addition of calcium chloride ($CaCl_2$) to initiate ionic crosslinking and form the hydrogel network. Several studies have also adopted this strategy to fabricate MOF–hydrogels for various sensing applications (listed in Table 1) [91, 94, 98, 100, 102, 107, 123–126].

2.1.3 | *Free-Radical Polymerization With Embedded MOFs*

The most widely used technique for fabricating hydrogels and their composites is free-radical polymerization. In this approach, free radicals initiate polymer chain growth in the presence of multifunctional crosslinkers, which react with the polymer chains to form covalent bonds and create a chemically crosslinked hydrogel network [127, 128]. When monomers such as acrylates, amides, and vinyl lactams are used to fabricate MOF–hydrogel composites for sensing applications, free-radical polymerization with embedded MOFs utilizes the functional groups of the monomers to initiate and propagate the polymer network. Two primary methods are commonly employed for free-radical polymerization: photo-initiated polymerization, in which light is applied in the presence of photo-initiators, and thermal-initiated polymerization, where catalysts are used to generate free radicals that initiate the polymerization process [129–132]. A representative study by Li et al. [118] demonstrated the fabrication of a single-network organohydrogel, reinforced with UiO-66-NH_2 MOF within polyacrylic acid (PAA) networks, to develop MOF–hydrogel composite-based electromechanical sensors. Ammonium persulfate was used as a thermal initiator to initiate free-radical polymerization by heating at 60°C for approximately 30 min, in the presence of *N,N′*-methylenebisacrylamide as a chemical crosslinker. Building on this approach, Liu et al. [133] further demonstrated the fabrication of a super-elastic MOF–hydrogel composite using a two-component thermal initiator system and catalysts to achieve rapid polymerization within minutes. In their study, various MOFs were physically incorporated into a pre-hydrogel solution, and instead of thermal initiation, polymerization was triggered by the addition of *N,N,N,N′*-tetramethylethylenediamine as a catalyst in the presence of ammonium persulfate, resulting in the rapid formation of a hydrogel network. For photo-initiated free-radical polymerization, a light-responsive photoinitiator generates free radicals upon exposure to ultraviolet or visible light, initiating the formation of the hydrogel polymer network. For example, Xia et al. [89] reported UiO-66 MOF-facilitated recyclable, ionic hydrogel-based sensors, where MOFs were incorporated into

TABLE 1 | Summary of MOF-embedded hydrogel composites with materials, fabrication methods, types of sensors, and sensing applications.

Hydrogel system	MOF component	MOF reinforced method	Hydrogel fabrication method	Type of sensor	Applications	Ref.
PEGDA	EuNDC	Physical embedding	UV-initiated free-radical polymerization	Optical	Healthcare, public safety	[89]
Agarose	UiO-66-NH_2	Physical embedding	Physical crosslinking	Optical	Environmental	[90]
SA	UiO-66-$(COOH)_2$	Physical embedding	Ionic crosslinking	Optical	Environmental	[91]
PAM–PVP	ZIF-8	Physical embedding	UV-initiated free-radical polymerization	Electromechanical	Healthcare, biomedical diagnostics	[92]
HAA	UiO-67-NH_2	Physical embedding	—	Optical	Healthcare, biomedical diagnostics	[93]
SA	Cu-TCPP(Co)	—	Ionic crosslinking	Optical	Healthcare, biomedical diagnostics	[94]
PAM	Tb-ZIF-8	Physical embedding	Thermal-initiated free-radical polymerization	Optical	Environmenal	[95]
Dodecyl methacrylate- PAM	Mn-Co-MOF	Physical embedding	Thermal-initiated free-radical polymerization	Electromechanical	Healthcare, electronics	[96]
SA	Eu(BTA)-Zr- MOF	Physical embedding	Physical crosslinking	Optical	Healthcare, biomedical diagnostics	[97]
Sodium carboxymethylcellulose	Cu-MOF	Physical embedding	Ionic crosslinking	pH	Healthcare, biomedical diagnostics	[98]
PAA	Fe-MIL-88NH_2	Physical embedding	Thermal-initiated free-radical polymerization	Electromechanical	Electronics	[99]
SA	Ce-Zr-MOF	Physical embedding	Ionic crosslinking	Optical	Environmental	[100]
Agarose	Fe-Co-MOF	—	Physical crosslinking	Optical	Healthcare, biomedical diagnostics	[74]
Agarose	NH_2-MIL-88(Fe)	Physical embedding	Physical crosslinking	Optical	Healthcare, biomedical diagnostics	[101]
SA	Eu-BDC	Physical embedding	Ionic crosslinking	Optical	Healthcare, biomedical diagnostics	[102]
Agarose	ZIF-8	Physical embedding	Ionic crosslinking	Optical	Healthcare, biomedical diagnostics	[103]
SA	Pb-MOF	Physical embedding	Ionic crosslinking	Optical	Environmental	[104]
SA	ZIF-8	Physical embedding	Ionic crosslinking	Optical	Environmental	[105]
PAM	Eu-MOF	Physical embedding	Thermal-initiated free-radical polymerization	Optical	Food safety, public health	[106]

(Continues)

TABLE 1 | (Continued)

Hydrogel system	MOF component	MOF reinforced method	Hydrogel fabrication method	Type of sensor	Applications	Ref.
SA	ZIF-8	Physical embedding	Ionic crosslinking	Optical	Healthcare, biomedical diagnostics	[107]
Gelatin	Zn-MOF	Physical embedding	Oil emulsion	Optical	Healthcare, biomedical diagnostics	[108]
PVP	MOF-71	Physical embedding	Lyophilization	Electrochemical	Healthcare, biomedical diagnostics	[109]
PVA–PVP	Fe-Co-MOF	Physical embedding	Lyophilization	Gas	Healthcare, environmental	[110]
PVA	Ni-Co-MOF	Physical embedding	Lyophilization	Electrochemical	Healthcare, biomedical diagnostics	[111]
PVA–CS	Fe-Co-MOF	Physical embedding	Lyophilization	Electrochemical	Healthcare, biomedical diagnostics	[73]
PAM–Starch	ZIF-8	In situ growth	Thermal-initiated free-radical polymerization	Optical	Healthcare, biomedical diagnostics	[112]
PAM–PEGDA	Cu-BTC	In situ growth	DLP 3D printing	Optical	Environmental	[113]
PAM–Cellulose	MOF-525	In situ growth	DIW 3D printing	Electromechanical	Healthcare, electronics	[114]
PAM–SA	Ce-BTC	In situ growth	DIW 3D printing	Optical	Healthcare, biomedical diagnostics	[115]
Lauryl methacrylate- PAM	Co-Mn-MOF	Physical embedding	Thermal-initiated free-radical polymerization	Electromechanical	Healthcare, electronics	[116]
Gelatin	UiO-67-NH_2	—	—	Optical	Environmental, biomedical diagnostics	[117]

an *N,N*-dimethylacrylamide (DMAA) hydrogel network, and 1-hydroxycyclohexyl phenyl ketone was used as an initiator under 365 nm UV light exposure to initiate free-radical polymerization. The procedure for fabricating MOF–hydrogel composites via free-radical polymerization, by physically incorporating or mixing MOFs and using either thermal or photo-initiated polymerization, is schematically illustrated in Figure 2B [118] and 2C [119], respectively. Several studies have also fabricated MOF–hydrogel composites using these methods, as comprehensively summarized in Table 1.

2.2 | In Situ Growth of MOFs Within Hydrogel Networks

In situ growth of MOFs within hydrogel networks is another method for fabricating MOF–hydrogel composites for sensing applications. Unlike approaches that embed pre-synthesized MOFs, this method involves the formation of MOF crystals directly within the preformed hydrogel matrix or during the gelation process itself [134–136]. The polymeric network of the hydrogel serves as a confined template or scaffold, providing nucleation sites that guide the crystallization and uniform dispersion of MOF particles throughout the matrix. As an example, Tian et al. [137] used an in situ growth approach to prepare MOF–hydrogel composite beads, which were successfully applied as moisture sensors. In their study, HKUST-1 crystals were generated within alginate hydrogel beads via an in situ self-assembly process, where Cu^{2+} ions coordinated with 1,3,5-benzenetricarboxylic acid (BTC) ligands inside the hydrogel network to form the MOF structure. Other studies have also employed in situ growth strategies combined with different polymerization techniques to fabricate MOF–hydrogel composites, as summarized in Table 1.

2.3 | Additive Manufacturing Approaches for MOF–Hydrogel Composites

Additive manufacturing, or 3D printing, offers precise control over architecture and material distribution and has emerged as a powerful tool for fabricating functional hydrogels [138–142]. However, its application in MOF–hydrogel composite fabrication remains largely unexplored. To date, only a few studies have reported the integration of MOFs into 3D-printed hydrogel matrices, and examples specifically targeting sensing and sensory systems remain scarce. A few studies, including work by Liu et al. [120], have fabricated flexible MOF–hydrogel composites using the direct ink writing (DIW) 3D printing technique. In their study, a copper (Cu)-based MOF, HKUST-1, was incorporated post-printing by first UV-curing the printed polyacrylamide (PAM) hydrogel structure, followed by swelling it in a MOF precursor solution to promote in situ growth of the MOF within the hydrogel network. Another study by Zhu et al. [113] employed a high-resolution digital light processing (DLP) 3D printing technique to fabricate Cu-BTC MOF–hydrogels for environmental sensing applications. An overall schematic of the 3D printing-based fabrication process for MOF–hydrogel composites is shown in Figure 2D [120], and the relevant studies are summarized in Table 1. Based on the foregoing analysis of MOF–hydrogel fabrication methods for sensors and sensing systems, most reported studies have employed the embedding of pre-synthesized MOFs into hydrogel matrices, whereas in situ growth and additive manufacturing remain comparatively underexplored for sensing applications. Although these strategies have advanced sensor development, significant challenges persist, including scaling to industrial production, ensuring structural and functional reproducibility, and minimizing batch-to-batch variability. As summarized in Table 2, physical embedding with different polymerization methods is valued for its operational simplicity, mild processing conditions, and broad compatibility with diverse MOFs, yet it is often limited by sedimentation, microstructural non-uniformity, and restricted scalability. In situ growth enables superior integration, enhanced homogeneity, and improved interfacial stability, though it requires precise reaction control and has yet to be widely implemented for large-scale fabrication. Additive manufacturing offers unparalleled opportunities for tailored architectures, geometric complexity, and multifunctional integration, but faces constraints related to rheology, printing resolution, and reliance on advanced printing platforms. Furthermore, large-scale MOF synthesis remains a critical bottleneck comparable to the early production challenges of graphene and carbon nanotubes, hindering broader application. Overcoming these manufacturing, reproducibility, and design limitations will be essential to fully exploit the synergistic potential of MOF–hydrogels in next-generation sensing technologies.

3 | MOF–Hydrogel Nanocomposites for Sensors and Sensing Platforms

The unique architecture and synergistic properties of MOF–hydrogel composites provide significant advantages for sensor design, enabling preconcentration, selective binding, sensitive detection of specific molecules, contaminants, volatile organic compounds, and various physical parameters. In recent years, numerous MOF–hydrogel-based sensors have already demonstrated exceptional performance in diverse application domains. Their design and fabrication are guided by theoretical insights, experimental findings, and structural characterization of the composite materials, which directly inform their functional properties and sensing performance. In the following sections, we review the structural strategies, advantages, and sensing principles of MOF–hydrogel-based sensors, along with their implementations for rapid and highly sensitive detection of physical, chemical, and biological stimuli across optical, electromechanical, electrochemical, and pH-responsive platforms.

3.1 | MOF–Hydrogel Nanocomposites in Optical Sensing

The integrated structure of MOF–hydrogel composites enables a broad spectrum of optical functionalities, including fluorescent, phosphorescent, colorimetric, plasmonic, and scintillating responses. Their diverse emission mechanisms encompass metal-centered luminescence in lanthanide-containing MOFs (LnMOF), typically arising from ligand-to-metal charge transfer, as well as exciplex/excimer emissions and ligand-derived luminescence [143–146]. Embedding MOFs within optically transparent, hydrated hydrogel networks not only preserves but often enhances their photophysical properties [147–150]. Furthermore, the hydrogel framework ensures homogeneous MOF distribution, biocompatibility, and responsiveness to external

TABLE 2 | Comparative analysis of advantages and disadvantages of MOF–hydrogel fabrication methods for sensors and sensing systems.

Fabrication method	Advantages	Disadvantages
Physical crosslinking with embedded MOFs	– Mild processing conditions preserve MOF crystallinity and surface chemistry. – Simple, low-cost, and solvent-free fabrication supports scalability and low production costs. – Uniform MOF dispersion before gelation ensures signal homogeneity across sensing surfaces.	– Limited control over network density and pore structure. – Susceptible to MOF leaching during operation, especially in aqueous environments. – Weak mechanical stability limits device durability in handling and operation. – Small batch and highly variable – Poor long-term shape retention in dynamic sensing setups. – Hard to achieve large-scale uniformity.
Ionic crosslinking with embedded MOFs	– Enables rapid, in situ hydrogel formation without heat or radical initiators. – Good compatibility with biological sensing platforms and delicate MOFs. – Ionically crosslinked networks can be formed directly on sensor substrates. – Facilitates high water content for analyte diffusion in sensing applications.	– Mechanical stability depends on environmental ionic strength. – Swelling/deswelling may alter embedded MOF distribution. – Limited structural precision for device miniaturization. – Potential interference from ions used in crosslinking during sensor operation.
Free-radical polymerization with embedded MOFs	– Strong covalent network improves robustness of sensor components. – High control over monomer composition for functional tailoring. – Scalable for complex or patterned sensor architectures. – Compatible with photolithography and additive manufacturing for integrated devices.	– Partially block MOF pores or alter surface chemistry. – Fabrication conditions (UV, heat, initiators) may degrade sensitive MOFs. – Requires photoinitiators or thermal initiators, adding cost and potential toxicity for biosensing. – One-pot molding limits complex geometries for sensor designs. – Long gelation times risk MOF sedimentation/agglomeration, causing non-uniformity and variable sensor performance.
In situ growth of MOFs within hydrogel networks	– Strong interfacial bonding between MOF and hydrogel matrix improves mechanical stability and sensing durability. – Controlled nucleation within the hydrogel ensures high MOF dispersion and signal uniformity. – Potential for hierarchical pore structures enhancing analyte diffusion and preconcentration. – Good reproducibility due to confined growth environment.	– Longer processing times and multiple synthesis steps can hinder scalability. – Metal ion or ligand diffusion limitations may cause gradients in MOF loading. – Requires precise reaction control to avoid non-uniform crystal size affecting signal reproducibility. – Specific reaction conditions and diffusion time make it slow for bulk production. – Difficult to run in high throughput without losing uniformity
Additive manufacturing or 3D printing of MOF–hydrogel composites	– Enables precise spatial control of MOF distribution for patterned or multi-functional sensors. – Facilitates fabrication of complex architectures for multi-analyte detection	– Longer processing times and multiple synthesis steps can hinder scalability. – Limited reports and processing protocols for MOF–hydrogel systems, especially for sensing.

(Continues)

TABLE 2 | (Continued)

Fabrication method	Advantages	Disadvantages
	or integration into flexible/wearable devices. – High design reproducibility ensures batch-to-batch consistency. – Digital fabrication allows rapid prototyping and direct customization for specific sensing needs.	– Printing resolution may be restricted by hydrogel viscosity and MOF particle size, with sedimentation, sagging, and agglomeration further affecting quality. – Scalability depends on the availability of high-throughput printing systems.

stimuli, making these composites well-suited for diverse optical sensing applications. The following subsections review key categories of MOF–hydrogel-based optical sensors, including luminescent, colorimetric, and plasmonic systems, highlighting their unique detection mechanisms and application potential.

3.1.1 | MOF–Hydrogel-Based Luminescent Sensor

Luminescence is the emission of light from a material following excitation by external energy sources such as photons, electrical input, or chemical reactions [151, 152]. Among its various forms, photoluminescence is the most common and is classified into fluorescence, a rapid emission from the excited singlet state, and phosphorescence, a delayed emission arising from spin-forbidden transitions between the triplet state and the ground state. In contrast, chemiluminescence represents a distinct type of luminescence that does not require external irradiation but instead results from chemical reactions that generate electronically excited species, which release light upon relaxation [153]. Luminescent sensors leverage these mechanisms to detect target analytes through changes in light intensity, wavelength, or lifetime, providing highly sensitive and selective readouts. Their non-invasive operation, fast response time, and capability for real-time detection make them particularly attractive for biomedical diagnostics, environmental monitoring, and food safety applications.

The luminescent properties of MOFs arising from their ligands, metal ions, guest species, or catalytic activity have been the most extensively exploited in MOF–hydrogel-based optical sensors [154–159]. Their chemically tunable frameworks and specific host-guest interactions enable the selective detection of metal ions, small organic compounds, or biomolecules. Coupled with their strong light-matter interaction, MOFs are particularly well-suited for fluorescence-based sensing. Embedding them within hydrogels provides additional benefits, including structural control, tunable porosity, and functional site modifications, enabling the creation of diverse and responsive luminescent sensors. MOFs also offer intrinsic biodegradability and compatibility with biological building blocks, enhancing their applicability in biomedical fields. Hydrogels complement these features by supplying optical transparency, uniform MOF dispersion, environmental protection, swelling capability, biocompatibility, and tissue-like mechanical properties. Together, these synergistic attributes have established MOF–hydrogel composites as versatile luminescence-based sensing platforms, surpassing traditional optical platforms in versatility and performance. Fluorescence remains the most widely exploited due to its high sensitivity and rapid response time, while chemiluminescence is emerging as a promising strategy by leveraging the catalytic activities of MOFs to amplify light emission during chemical reactions.

The sensing performance of these systems primarily relies on host-guest interactions with analytes, which trigger measurable luminescence changes such as intensity modulation, including turn-on or turn-off effects and or emission peak shifts. Representative mechanisms include photo-induced electron transfer (PET), intermolecular charge transfer (ICT), and fluorescence resonance energy transfer (FRET). A comprehensive overview of these mechanisms is available in reviews by Yan and colleagues [160].

Among these mechanisms, fluorescence quenching has been most widely exploited, typically using luminescent MOFs with emissive metal centers. For example, Zhao et al. [89] developed a europium (Eu) based MOF–hydrogel optical fiber as a novel platform for photoluminescent sensing of picric acid, a nitroaromatic explosive compound. Water and thermally stable luminescent EuNDC MOFs (NDC = 1,4-naphthalene-dicarboxylic acid) were embedded within poly(ethylene glycol) diacrylate (PEGDA) hydrogel matrices to enable real-time, on-site monitoring. The core-clad fiber design, featuring a step-index profile, facilitated efficient propagation of excitation light and collection of emission signals. Additionally, embedding the MOFs within the hydrogel core not only protected them from direct exposure to harsh environments, thereby preventing leakage of luminescent particles, but also preserved open channels for analyte diffusion. This configuration enhanced the sensor's operational stability and longevity. By combining the photoluminescent properties of MOFs with the optical transparency and flexibility of hydrogels, the system demonstrated high sensitivity, with fluorescence quenching visibly detectable at picric acid concentrations as low as 5.7 ppm.

In another example, a fluorescence-quenching-based sensing platform was constructed using a modified MOF embedded within a photo-crosslinked hydrogel matrix [161]. Specifically, UiO-66-NH_2 MOF was post-synthetically modified via aldimine condensation with 2,3,4-trihydroxybenzaldehyde to yield fluorescent material (Figure 3A) [161]. Subsequent coordination with Fe^{3+} produced modified UiO-66-NH_2 MOF, which exhibited quenched fluorescence due to Fe^{3+} binding. In the presence of bilirubin, which has a strong affinity for Fe^{3+}, the ions were displaced, leading to fluorescence recovery and enabling a turn-on sensing response (Figure 3B) [161]. To enhance detection performance and usability, post-synthetically modified MOF was embedded within a photo-crosslinked gelatin methacryloyl (GelMA) hydrogel, forming a GelMA-functionalized MOF

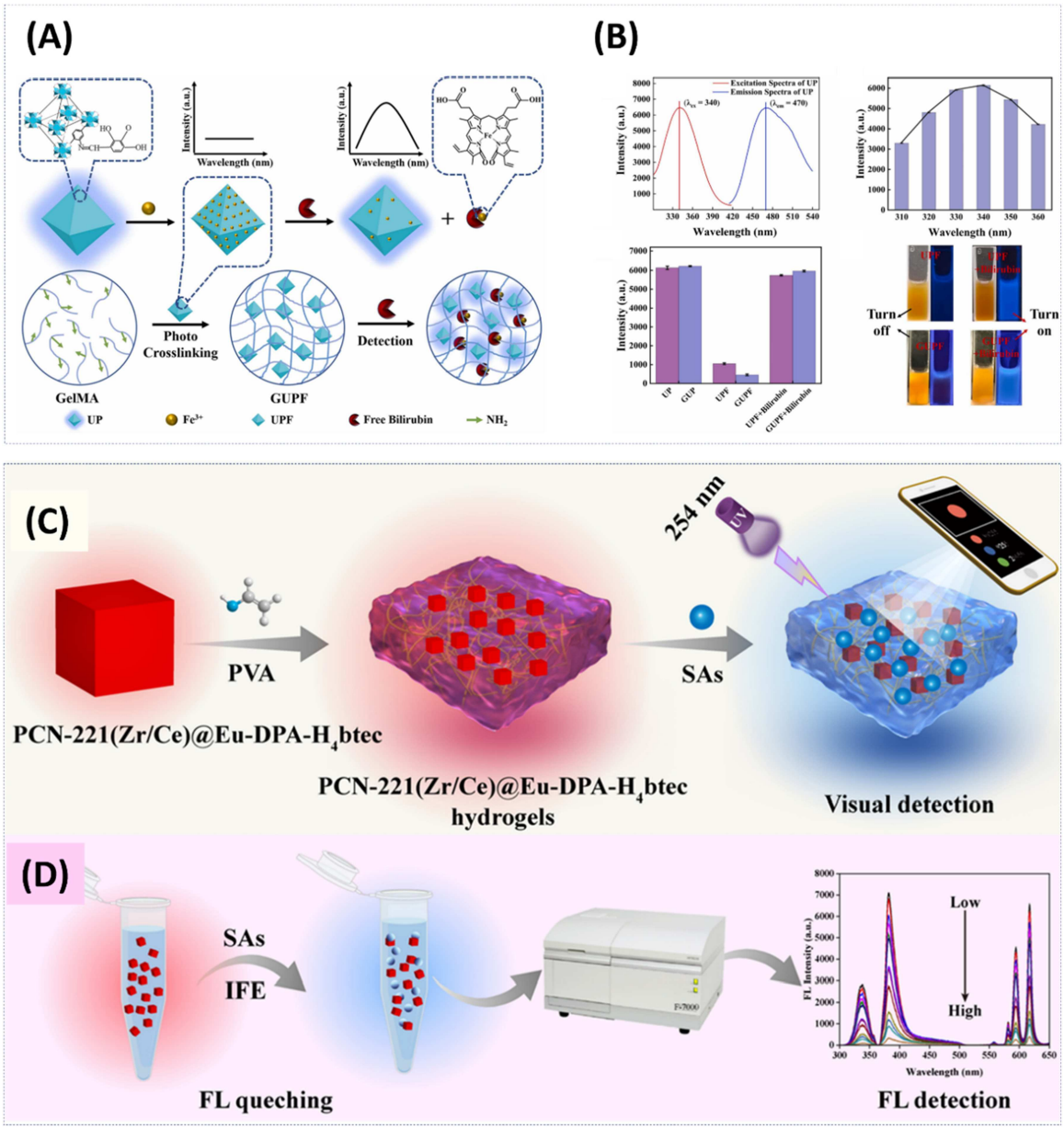

FIGURE 3 | MOF–hydrogel-based optical luminescence sensors. (A) Schematic illustration of a fluorescence-quenching-based sensing platform constructed using UiO-66-NH_2 MOF embedded in a photocrosslinkable GelMA hydrogel. Reproduced with permission: Copyright 2024, Elsevier [161]. (B) Fluorescence characterization of the UiO-66-NH_2-integrated GelMA hydrogel system, showing excitation/emission behavior, Fe^{3+} induced quenching, bilirubin-responsive fluorescence recovery, and visible fluorescence changes under daylight and UV light. Reproduced with permission: Copyright 2024, Elsevier [161]. (C) Schematic diagram of visual detection using a ratiometric fluorescence sensor based on a PCN-221(Zr/Ce)@Eu-MOF-incorporated hydrogel. Reproduced with permission: Copyright 2024, Elsevier [76]. (D) Schematic illustration of the sensing mechanism for sulfonamide detection using the proposed PCN-221(Zr/Ce)@Eu-MOF-based ratiometric fluorescence sensor. Reproduced with permission: Copyright 2024, Elsevier [76].

composite. This hybrid hydrogel composite provided a stable, biocompatible, and porous matrix that promoted bilirubin enrichment at the sensing interface, thereby amplifying the fluorescence response. The resulting sensor achieved an ultralow detection limit of 5.67 pM and demonstrated excellent performance in real human urine samples. Several additional studies have also adopted MOF–hydrogel-based optical luminescence sensors utilizing fluorescence quenching mechanisms for the detection of various environmentally and biologically relevant analytes, as systematically summarized in Table 3 [74–80, 82–84, 89, 91, 94, 102–106, 123, 125, 161–166].

In a separate approach, a luminescent MOF–hydrogel film-based portable sensor array was developed by Wang et al. [91] for the selective detection of nitrophenol isomers. The sensor integrated Eu^{3+} and terbium (Tb^{3+}) ions into a mixed-ligand luminescent MOF, specifically Eu^{3+}/Tb^{3+}@UiO-66-$(COOH)_2$/NDC, which was embedded within a SA hydrogel matrix to create three distinct luminescence centers. This configuration enabled discrimination among *o*-nitrophenol, *m*-nitrophenol, and *p*-nitrophenol isomers using linear discriminant analysis. The fluorescence resonance energy transfer-based sensing mechanism relied on differential quenching of Eu^{3+} and Tb^{3+}

TABLE 3 | Summary of MOF-based hydrogel optical sensors, including sensing mechanisms, sensing parameters, target analytes, and limits of detection.

Composition	Sensor type	Sensing mechanism	Sensing parameters	Target analyte	LOD	Ref.
EuNDC–PEGDA	Photoluminescence	Fluorescence quenching	Fluorescence emission intensity	Picric acid	5.7 ppm	[89]
SA–UiO-66-$(COOH)_2$	Luminescence	FRET	Fluorescence emission intensity	Nitrophenol	40–100 μM	[91]
Agarose–MnO_2@ZIF-8	Luminescence	Fluorescence resonance energy transfer	Fluorescence emission intensity	Alanine amino-transferase	0.5 U/L	[103]
SA–Eu^{3+}-ZnMOF	Luminescence	pH-responsive structure and antenna effect	Fluorescence emission intensity	Aspartic acid & arginine	—	[82]
SA–EuBDC	Luminescence	"ON-OFF-OFF-ON" fluorescence transition trigger	Luminescent intensity	β-Lactamase	1.25 U/mL	[102]
SA–Au@ZIF-8	Luminescence	Fluorescence quenching	Fluorescence emission intensity	Copper ions & organo-phosphorus	0.016 μM	[105]
PHEMA–EuMTA	Luminescence	Fluorescence quenching	Fluorescence intensity	Ferric ions	2 ppm	[162]
PEGDA–Eu-MOF	Luminescence	Fluorescence quenching	Fluorescence intensity	Cortisol	1 nM	[79]
GelMA–UiO-66-NH_2	Luminescence	Fluorescence quenching	Fluorescence intensity	Bilirubin	5.67 pM	[161]
PVA–SA-LnMOF	Luminescence	Fluorescence quenching	Fluorescence intensity	Aldehyde	0.22 ppm	[163]
Carrageenan-Ru@UiO-OH	Ratiometric fluorescence	LMCT and ESIPT	Fluorescence intensity	Trimethylamine	Not specified	[83]
PAM–EuMOF	Ratiometric fluorescence	Energy and the ligand-to-metal charge transfer	Fluorescence intensity & visual detection	Glyphosate	0.35 mg/L	[106]
PVA–PCN-221(Zr/Ce)@Eu	Ratiometric fluorescence	FRET and electron transfer	Fluorescence intensity	Sulfonamides	45 nM/L	[76]
SA–CDs@Eu-UiO-67b	Ratiometric fluorescence	Fluorescence quenching via internal filter effect	Fluorescence intensity	Ofloxacin & tetracycline	22–27 nM	[123]
Eu-MOF@PVA	Ratiometric fluorescence	FRET	Fluorescence intensity	Carcinoid	37.16 nM	[80]
Eu-BOP/BDC-OH	Ratiometric fluorescence	Fluorescence quenching via internal filter effect	Fluorescence intensity	Histamine	0.17 mg/L	[164]
Carrageenan-Eu-BOP/BDC-OH	Chemiluminescence	Signal-on chemiluminescence	Chemiluminescence intensity	Thrombin	0.2178 pM/L	[94]
CS@Pt-MOF	Chemiluminescence	Catalase-like activity	Chemiluminescence intensity	Organophosphorus & D-amino acids	0.21 ng/mL & 0.12 μM	[75]
Agarose-Au@Co-Fe-MOF	Colorimetric	Peroxidase-like catalytic activity	Absorbance	Isoniazid	0.2 μM	[74]
Agarose@Cu-hemin	Colorimetric	Peroxidase-like catalytic activity	Absorbance	Glucose	2.8 μM	[77]

(Continues)

TABLE 3 | (Continued)

Composition	Sensor type	Sensing mechanism	Sensing parameters	Target analyte	LOD	Ref.
HAA–MOFzyme	Colorimetric	Peroxidase-like catalytic activity	Absorbance	Sarafloxacin	2.06 pg/mL	[84]
Agarose–UiO-66(Fe/Zr) -NH_2	Colorimetric	Peroxidase-mimicking activity	Absorbance	Kanamycin & oxytetracycline	0.44 nM	[78]
SA–AuNCs@Pb-MOF	Colorimetric and fluorescence	Electronic structure disruption & fluorescence quenching	Fluorescence intensity & visible color change	H_2S	5.4 μM	[104]
SA–Au@Cu -MOF	SERS	Schiff base reaction	Raman intensity	Putrescine	0.63 nM/L	[125]
PEGDA–Plasmonic MOFs	SERS	Surface plasmon resonance	Raman intensity	Acetaminophen	0.45 μM	[165]
PVA–UiO-66- NH_2	SERS	Localized surface plasmon resonance	Raman intensity	Kanamycin	0.158 pM	[166]

emissions upon interaction with each isomer, generating unique optical signatures for statistical analysis. The lanthanide-based MOFs provided sharp, stable dual-emission properties, while the hydrogel contributed flexibility, optical transparency, and efficient analyte diffusion. This composite system demonstrated excellent portability, environmental stability, and selective sensing performance. It successfully detected nitrophenol isomers at concentrations ranging from 40 to 100 μM, enabled semi-quantitative analysis in the 0 to 80 μM range, and distinguished binary and ternary mixtures at 60 μM. This fluorescence resonance energy transfer-based sensing mechanism was also employed in the development of another MnO_2@ZIF-8-luminol MOF–hydrogel-based sensor for the fluorescence detection of alanine aminotransferase [103].

Building on similar MOF–hydrogel integration strategies, Sha et al. [82] developed a dual-emission MOF–hydrogel hybrid film for selective amino acid sensing. The system was fabricated by embedding Eu^{3+}-functionalized zinc-based MOFs into an SA-based hydrogel network. The Zn-MOF contained uncoordinated carboxyl groups that provided binding sites for Eu^{3+} ions, forming luminescent centers within the hydrogel. Under acidic conditions, the composite film exhibited distinct fluorescence responses, enabling the detection of aspartic acid and arginine. This pH-responsive behavior, coupled with the antenna effect of $Eu^{3+,}$ contributed to the sensor's high selectivity and semi-quantitative detection capability. Additionally, the tunable fluorescence shifts in response to target analytes were utilized to fabricate fluorescent hydrogel films for anti-counterfeiting and information security applications. Notably, the study did not report the limit of detection (LOD) for the analytes but emphasized the qualitative and semi-quantitative potential of the system under controlled pH environments.

In a related study, Lian et al. [102] developed a luminescent MOF–hydrogel composite sensor by embedding Zr-based PCN-224 MOFs into SA for detecting β-lactamase, a biomarker associated with penicillin allergy. This system employed a unique "ON-OFF-OFF-ON" fluorescence switching mechanism initiated by enzymatic hydrolysis of a β-lactam ring. The hydrogel ensured analyte accessibility and biocompatibility, while the MOF served as a robust fluorescent core. The sensor achieved a low LOD of 1.25 U/mL for β-lactamase and could also detect penicillamine with high sensitivity, demonstrating potential for point-of-care diagnostics with visual fluorescence readouts.

Another simple yet effective strategy was employed to develop a ratiometric fluorescence sensor by incorporating dual-emissive MOF probes into a color-transition hydrogel [83]. Specifically, functionalized Ru@UiO-OH (Ru=Ruthenium) MOFs were embedded within a carrageenan matrix for the visible and selective detection of biogenic amines. Upon exposure to trimethylamine, the fluorescence intensities exhibited distinct changes under a single excitation wavelength, resulting in a ratiometric signal and a noticeable color shift from orange-red to bright yellow. This "turn-on" yellow emission was attributed to the inhibition of ligand-to-metal charge transfer (LMCT) and excited-state intramolecular proton transfer (ESIPT) processes, both affected by MOF framework degradation and ligand deprotonation. The Ru@UiO-OH-loaded hydrogel served as a "sniffing" indicator for volatile trimethylamine vapor and was further coupled with a smartphone-based platform for real-time, quantitative visual analysis. To support user-friendly field deployment, Jie et al. [76] proposed a

Eu-postfunctionalized porphyrin-based trimetallic PCN-221 (Zr/Ce)@Eu-MOF–hydrogel for visual ratiometric fluorescence sensing of sulfonamides in food samples. This trimetallic MOF and PVA-based hydrogel fluorescent biosensor employed inner filter effect, FRET, and electron transfer as the sensing mechanisms, illustrated in Figure 3C,D [76]. It offered a convenient, rapid, and efficient approach for detecting antibiotic residues in raw pork and milk samples, achieving a low LOD of 45 nM/L and satisfactory recovery rates. Similarly, another ratiometric fluorescent sensing platform, integrated with both a paper-based sensor and a skin-attachable hydrogel, was developed using enoxacin-embedded EuMOF for user-friendly detection of glyphosate [106]. This platform demonstrated excellent sensitivity, achieving a LOD of 0.35 mg/L for fluorescence-based detection and 10 mg/L for visual detection. Similarly, Liu et al. [123] developed a ratiometric fluorescence sensor by incorporating carbon dots and Eu^{3+}-modified UiO-67b into a SA hydrogel for monitoring ofloxacin and tetracycline residues, achieving a detection limit of 22–27 nM. Additionally, several other studies have reported MOF–hydrogel-based ratiometric fluorescence sensors for various applications [80, 167].

As an alternative to fluorescence mechanisms, another study introduced a "signal-on" chemiluminescence biosensor for thrombin detection by integrating metalloporphyrinic MOF nanosheets (Cu-TCPP(Co)) with a DNA-functionalized magnetic SA hydrogel [94]. In this system, the hydrogel served as a capture matrix for thrombin via aptamer interactions and was subsequently dissolved with EDTA to release the bound target. The released complex activated the chemiluminescent reaction, with the MOF acting as a catalytic signal enhancer. Upon specific thrombin recognition, the MOF-Au-ssDNA complex was liberated, resulting in amplified light emission. This biosensor exhibited excellent sensitivity, achieving a detection limit of 0.2178 pM/L and a broad linear range from 0.893 to 595.6 pM/L. Building on this chemiluminescence strategy, Lu et al. [75] reported another hydrogel-based sensor that employed platinum (Pt) MOFs to achieve long-lasting chemiluminescence imaging for the detection of pesticides and D-amino acids. Inspired by the persistent luminescence of hydrogels and the highly stable catalase-like activity of MOF-Pt, they constructed a glow-type chemiluminescence imaging sensor using a long-lasting *N*-(4-aminobutyl)-*N*-ethylisoluminol/Co^{2+}/CS hydrogel system. The high viscosity of the hydrogel matrix slowed molecular diffusion, prolonging the chemiluminescence emission, while the catalytic activity of MOF-Pt enhanced the signal intensity by sixfold. This synergistic effect enabled sensitive quantification of chlorpyrifos with a detection limit of 0.21 ng/mL, and D-alanine in serum with an LOD of 0.12 μM. These examples collectively demonstrate the broad applicability and strong potential of MOF–hydrogel composites in the field of optical sensing. Their unique combination of tunable luminescent properties, structural flexibility, and biocompatibility offers a powerful platform for the development of next-generation optical sensors. By integrating the dynamic responsiveness of hydrogels with the highly customizable photophysical characteristics of MOFs, these hybrid systems can be engineered to achieve multifunctionality, high sensitivity, and selectivity.

3.1.2 | *MOF–Hydrogel-Based Colorimetric Sensor*

Colorimetric sensors are analytical devices that detect and quantify target analytes through a visible color change. This optical response, often perceivable with the naked eye, arises from chemical or biochemical reactions and eliminates the need for complex instrumentation [168]. The observed color change typically results from alterations in molecular structure, oxidation state, or the aggregation behavior of chromogenic agents upon interacting with specific analytes. Among various optical sensing approaches, colorimetric sensing has attracted considerable attention due to its low cost, fast response time, and straightforward visual interpretation [169]. These features make colorimetric sensors especially suitable for use in portable or on-site applications, where access to advanced equipment and trained personnel may be limited. When integrated into MOF–hydrogel systems, colorimetric sensors leverage the high porosity, tunable functionalities, and selective adsorption characteristics of MOFs, significantly enhancing their sensitivity and analyte specificity [170]. Although substantial progress has been made in developing colorimetric sensors based on MOFs alone, their integration into hydrogel matrices remains in its early stages, with only a limited number of MOF–hydrogel-based colorimetric sensors reported to date.

Recently, Yu et al. [74] developed a hydrogel-based colorimetric sensing platform integrated with a smartphone for the detection of isoniazid in human urine and serum. The system utilized gold nanoparticle (AuNP)-functionalized bimetallic MOF nanozymes (NMOF-Co-$Fe_{1.8}$), which mimic peroxidase activity to catalyze the oxidation of 3,3′,5,5′-tetramethylbenzidine in the presence of hydrogen peroxide, yielding a blue-colored product. Isoniazid inhibited this reaction, yielding a concentration-dependent decrease in color intensity. The sensor exhibited a linear detection range of 0.25–120 μM with a low detection limit of 0.2 μM, and it demonstrated excellent recovery (97.0%–103.7%) along with high reproducibility, as indicated by relative standard deviations (RSD < 3%). Similarly, Lin et al. [77] exploited peroxidase-like catalytic activity based on Cu-hemin-MOF embedded in an agarose hydrogel for glucose detection. Another example involved a colorimetric aptasensor in which catalase was encapsulated within MOF cavities and integrated into a nucleic acid hydrogel for selective sarafloxacin detection [84].

Building on these colorimetric designs and the peroxidase-mimicking paradigm, Nie et al. [104] introduced a gold nanocluster (AuNC)-embedded MOF as a dual-channel hydrogel optical sensor for simple, efficient, and real-time monitoring of hydrogen sulfide (H_2S). To address prior challenges such as limited anti-interference capacity, inadequate selectivity, and operational complexity, the study employed a bottle-around-ship approach to encapsulate AuNCs within lead (Pb)-based MOFs. Embedding the AuNCs@Pb-MOF into a dual-channel SA hydrogel with high porosity and optical transparency significantly enhanced the sensor's luminescence efficiency and stability (Figure 4A) [104]. This compact and portable sensor combines fluorescence and colorimetric detection modes, offering a low detection limit of 5.4 μM, rapid response time (<30 s), strong interference resistance, and seamless compatibility with smartphone-based analysis systems. These recent developments suggest the emerging potential of MOF–hydrogel composites in colorimetric sensing platforms. Continued innovation in MOF design and hydrogel integration is expected to broaden their applicability across diverse biomedical and environmental domains.

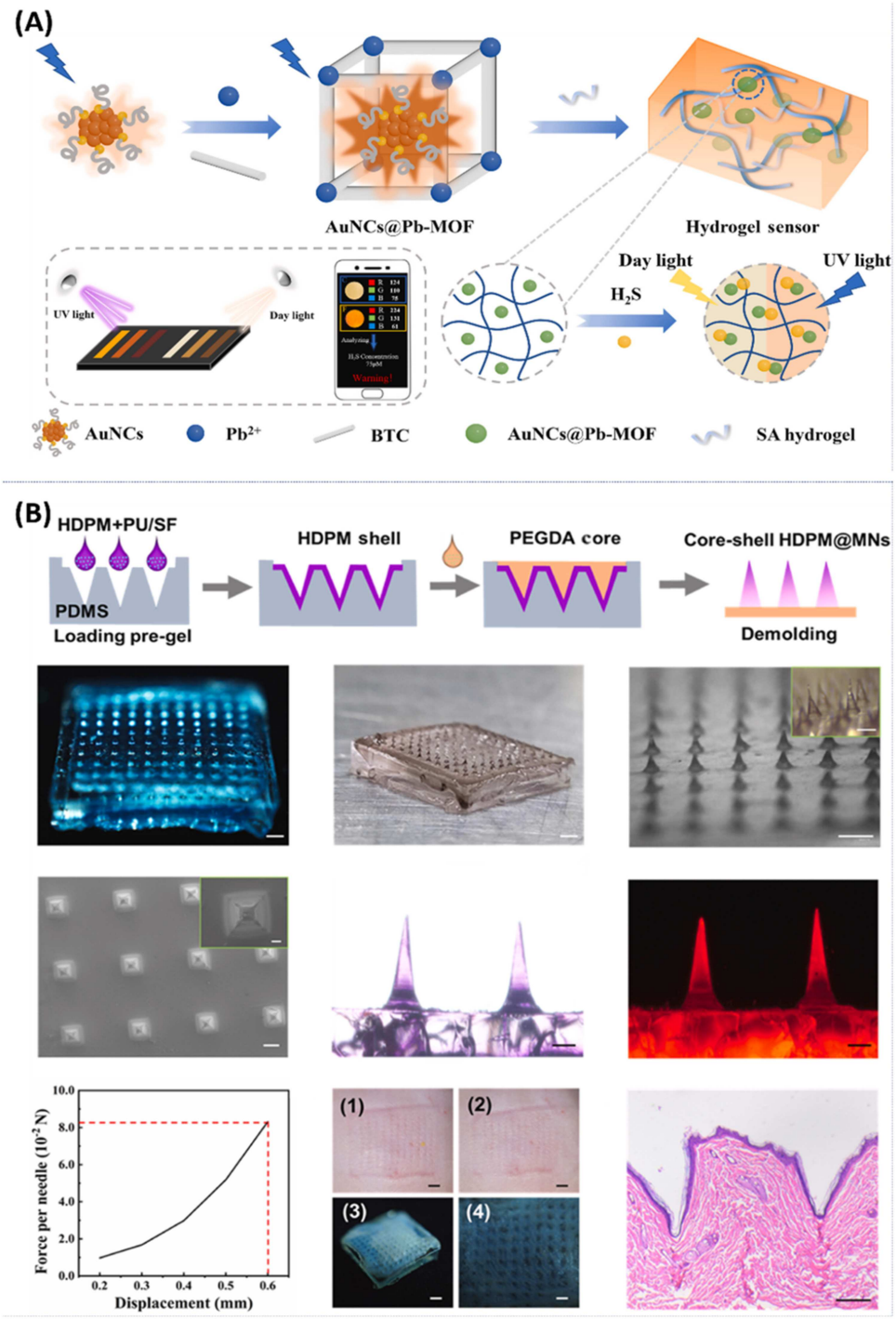

FIGURE 4 | (A) Schematic illustration of a dual-channel SA hydrogel-based optical colorimetric sensor constructed using gold nanocluster-embedded Pb-MOF for sensitive and visual detection applications. Reproduced with permission: Copyright 2025, Elsevier [104]. (B) Corn-inspired high-density plasmonic MOF–hydrogel-based microneedle sensor for non-destructive monitoring of biological analytes via surface-enhanced Raman scattering. Reproduced with permission: Copyright 2024, Elsevier [165].

3.1.3 | *MOF–Hydrogel-Based SERS Sensor*

Complementing luminescence-based and colorimetric strategies, plasmonic sensing via surface-enhanced Raman spectroscopy (SERS) provides an additional pathway for optical detection. SERS is a vibrational technique that enables ultrasensitive detection of low-concentration analytes by amplifying electromagnetic fields through localized surface plasmon excitation [171]. SERS typically relies on noble metals such as Au and Ag, whose strong plasmonic coupling greatly enhances Raman scattering. By contrast, MOFs by themselves are non-plasmonic. They provide adsorption capacity and selectivity but cannot create the required electromagnetic hot spots, so effective MOF-based SERS pairs them with plasmonic metals. Nevertheless, functionalizing MOFs with plasmonic materials has shown great promise. Their high surface areas and microporosity provide abundant adsorption sites and selective size screening, thereby enhancing sensitivity and enabling single-molecule detection.

Several MOF–hydrogel-based plasmonic hybrids have recently been proposed. Li et al. [165] reported a corn-inspired high-density plasmonic MOF–hydrogel-based microneedle sensor for non-invasive SERS monitoring of interstitial fluid analytes. The device integrated MIL-101, an Fe-based MOF, with densely packed Au nanospheres on a PEGDA hydrogel core to form a hybrid SERS-active substrate (Figure 4B) [165]. This architecture combines a large specific surface area, hierarchical porosity, and strong electromagnetic field enhancement, yielding efficient analyte enrichment and highly sensitive detection. The microneedle format allowed skin penetration with minimal tissue damage while maintaining structural integrity, achieving a detection range of 1–100 μM with a LOD of 0.45 μM for acetaminophen.

In a related study, Cao et al. [125] developed a SERS-active hydrogel nanoreactor by embedding Au nanobowls within a Cu-MOF layer supported on a sodium alginate hydrogel scaffold. This hybrid material was employed for the highly specific and sensitive detection of putrescine, a biogenic amine linked to food spoilage. The Cu-MOF component selectively captured putrescine, while *o*-phthalaldehyde reacted with the analyte to form a Raman-active Schiff-base complex positioned at the MOF–hydrogel interface, which enabled strong signal amplification. The sensor achieved ultralow detection limits of 1.2 nM in gaseous samples and 0.63 nM in liquid samples, along with excellent selectivity against common interfering molecules. More recently, an intelligent dual-mode sensing platform was engineered by incorporating Au nanostructures, Prussian Blue nanozymes, and DNA aptamers within a MOF–hydrogel matrix [166]. This system was applied for SERS and colorimetric detection of kanamycin, where MOFs acted as gated reservoirs for tetramethylbenzidine and aptamers provided selective recognition. The platform achieved ultralow detection limits, high specificity, and demonstrated strong potential for integration into portable antibiotic monitoring devices. In particular, the sensor enabled ultrasensitive kanamycin identification with a detection limit of 0.158 nM and a broad linear range from 1 nM to 1000 μM across both colorimetric and Raman modes. Together, these findings underscore the potential of the MOF–hydrogel plasmonic hybrid for advanced SERS sensing. They also highlight the limitations of standalone MOFs or hydrogels, which often lack the necessary plasmonic enhancement or molecular recognition capabilities required for high-performance SERS-based optical sensing applications.

3.2 | MOF–Hydrogel Nanocomposites in Electrochemical Sensing

Electrochemical sensors are analytical devices that detect specific analytes through selective interaction with a sensing element [172, 173]. The interaction generates a response that is converted into an electrical signal by a transducer, with the signal intensity reflecting analyte concentration. These devices can be classified into potentiometric, amperometric, voltammetric, impedimetric, and conductometric sensors, depending on whether they measure ion concentration, current, impedance, or conductivity [174].

MOFs and hydrogels possess distinct yet complementary properties that make them highly attractive for electrochemical sensing. MOF derivatives provide high surface area, well-defined porosity, and structural tunability, which facilitates access to active sites and selective analyte interaction, enhancing sensitivity and selectivity [175–177]. Hydrogels, in turn, offer hydrated, biocompatible 3D networks that undergo volumetric, ionic, or conductivity changes in response to external stimuli [178–180]. Integrating MOFs into hydrogel matrices combines these advantages, yielding versatile, transducer interfaces with improved sensitivity, lower detection limits, enhanced signal stability, and adaptability to complex environments, including wearable and in vivo systems.

A notable example was reported by Liu et al. [181], who developed a smartphone-compatible electrochemical sensor for adrenaline detection. The device employed microspherical bimetallic Co-Ni MOFs embedded within a CS-PAM hydrogel network (Figure 5A) [181]. This architecture synergistically combined the high surface area and redox activity of MOFs with the ionic conductivity, mechanical flexibility, and hydrophilicity of the hydrogel. The catalytic properties of the hydrogel matrix were tuned by varying MOF loading, producing a hierarchically structured material with enhanced electrocatalytic performance. The optimized sensor exhibited dual linear detection ranges (0.5–10 and 10–2500 μM), a remarkably low detection limit of 0.167 μM, and high sensitivity values of 0.182 and 0.133 μA μM/cm^2. It also demonstrated stability across 60 repeated measurements, excellent selectivity against common interferents, and efficient charge transfer with abundant electroactive sites. This study highlights the ability of MOF–hydrogel composites to fine-tune electrocatalytic interfaces for portable bioanalytical platforms. Building on this approach, Sun et al. [182] created a hybrid electrochemical sensor by incorporating rigid MOF nanocrystals into a CS-PAM supramolecular hydrogel. The composite consisted of a MIL-88 B MOF containing Fe and Cu, coated with a covalent organic framework (COF) shell (Figure 5B) [182]. The resulting MOF–COF-Hydrogel system enabled highly sensitive and selective detection of noradrenaline bitartrate. The hydrogel matrix improved MOF/COF dispersion, provided diffusion pathways, and contributed ionic conductivity, while the COF shell supplied π–π interactions. The sensor achieved a wide linear range (0.06–1600 μM), a low LOD (0.02 μM), and excellent selectivity, stability, and repeatability, without requiring sealing agents.

Another innovative design integrated MOF-71 with vanadium carbide MXene (V_2C MXene) into a porous, hydrophilic hydrogel via a solvothermal and freeze-drying process [109]. This hybrid material was employed for the simultaneous electrochemical detection of levothyroxine (LT4) and carbamazepine (CBZ) in simulated blood serum. The MOF-MXene hydrogel exhibited a broad linear detection range (10 nM–100 μM for LT4 and 10 nM–500 μM for CBZ) with low detection limits (5.6 nM for LT4 and 6.7 nM for CBZ). It further demonstrated excellent selectivity against common interfering species and high reproducibility, with RSD of 1.65% for LT4 and 2.81% for CBZ. These results were attributed to the hydrogel's high ion mobility, enhanced electrochemical activity, and stable electrode interfacing, which together enabled sensitive and selective detection in complex biological environments. Such properties highlight the potential of MOF-MXene hydrogels for integration into wearable and portable diagnostic platforms.

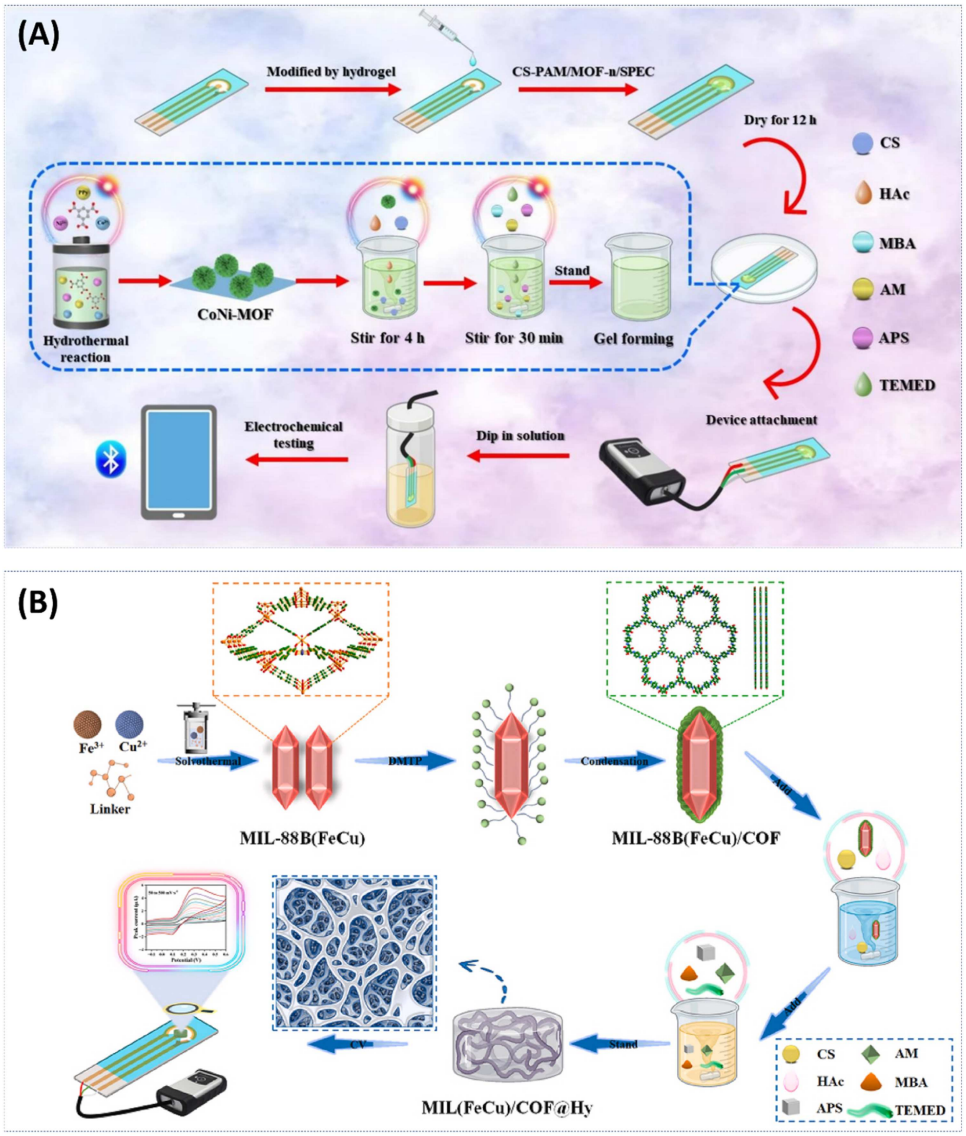

FIGURE 5 | (A) Schematic illustration of a portable smartphone-based adrenaline sensing platform constructed using microspherical bimetallic Co-Ni MOF and CS-PAM hydrogel composites. Reproduced with permission: Copyright 2024, Elsevier [181]. (B) A portable electrochemical sensing platform for noradrenaline bitartrate detection using a bimetallic Fe-Cu integrated hydrogel-modified screen-printed electrode. Reproduced with permission: Copyright 2024, Elsevier [182].

Despite these advances, research on MOF–hydrogel electrochemical sensors remains relatively limited, with only a few studies involving bimetallic MOFs reported to date. These representative examples are summarized in Table 4 [73, 85, 109, 111, 181–189].

3.3 | MOF–Hydrogel Nanocomposites in Electromechanical Sensing

Electromechanical sensors have attracted significant attention as key technologies for converting mechanical stimuli into measurable electrical signals. They underpin many emerging applications in flexible and wearable electronics, human–machine interfaces (HMIs), healthcare monitoring, and soft robotics [190, 191]. By transducing external stimuli such as pressure, strain, or motion into electrical outputs, electromechanical sensors enable real-time interaction with the surrounding environment. Based on their signal transduction mechanisms, they are typically classified into four main categories: piezoresistive, piezocapacitive, piezoelectric, and triboelectric nanogenerator (TENG) sensors, each offering distinct advantages in terms of sensitivity, response speed, energy efficiency, and fabrication compatibility. As technological demands continue to evolve, the development of advanced functional materials such as MOF–hydrogel composites has opened new pathways for designing high-performance and multifunctional electromechanical sensors. This section outlines the fundamental principles of electromechanical sensing and introduces recent progress in MOF–hydrogel-based sensor platforms.

Hydrogels have been widely used in electromechanical sensors owing to their exceptional properties, including mechanical stretchability, flexibility, skin-like compliance, recoverability, and responsiveness to multiple stimuli [47]. Their ability to incorporate salts provides ionic conductivity, making them highly suitable for conductive sensing platforms. While

TABLE 4 | Summary of electrochemical sensing methods, mechanisms, and performance metrics for MOF–hydrogel-based sensors.

Composition	Method	Sensing mechanism	Target analyte	Sensitivity	Linear range	LOD	Ref.
PVA/CS-Fe/Co-MOF	Square wave voltammetry	Electrochemical oxidation	Lactic acid	0.02 mA mM/cm^2	0.05 μM–100 mM	0.01 μM	[73]
Graphene hydrogel-Mn–ZIF-8	Differential pulse voltammetry	Electrochemical oxidation-reduction	Trolox	—	0.01–103.79 μM	0.08 μM	[85]
PVA@NiCo Ni-MOF	Differential pulse voltammetry	Electrochemical catalytic oxidation	Urea	—	0.5–70 mM	0.445 mM	[111]
CS–PAM@CoNi-MOF	Differential pulse voltammetry	Electrocatalytic oxidation	Adrenaline	0.133 μA μM/cm^2	0.5–10 & 10–2500 μM	0.167 μM	[181]
PAM@Fe-MOF	Square wave voltammetry	Mass & electron transfer modulation	H_2O_2	—	0.001–100 ng/mL	14.24 fg/mL	[183]
CS–SA@UiO-66-NH_2	Differential pulse voltammetry	—	Chlorogenic acid	0.06 μA μM/cm^2	0.1–1000 μM/L	0.03 μM/L	[184]
CS–Guar gum@CuNi-MOF	Differential pulse voltammetry	Electrocatalytic oxidation	Acetaminophen		0.07–1500 μM	0.023 μM	[185]
PVA@ZnS/MnO_2-MOF	Differential pulse voltammetry	Electro-oxidation	Glutathione	8.45 μA nM/cm^2	10 nM–10 mM	6.88 nM	[186]
PVA@MOF-71/V_2C MXene	Differential pulse voltammetry	Electro- oxidation	Levothyroxine & carbamazepine	—	10 nM–100 μM & 10 nM–500 μM	5.6 & 6.7 nM	[109]
PAM@MIL-88B (FeCu/COF)	Differential pulse voltammetry	Electrocatalytic oxidation	Noradrenaline bitartrate	0.064 μA μM/cm^2	0.06–10 μM/L & 10–1600 μM/L	0.02 μM/L	[182]
CS–PAM@Cu-MOF	Differential pulse voltammetry	Mass & electron transfer modulation	Aflatoxin B1	—	0.001–100 ng/mL	0.0003 ng/mL	[187]
PAM–PVA@Ni-HAB	Differential pulse voltammetry	Electrocatalytic oxidation	Dopamine	0.47 μA μM/cm^2	0–285 μM	18 nM	[188]
SA-CS@MIP-Cu-MOF	Differential pulse voltammetry	—	Chelerythrine	—	50–500 nM/L	13.8 nM/L	[189]

composites of hydrogels with carbon-based nanofillers have been extensively studied, MOF–hydrogel composites remain relatively underexplored, primarily due to the predominantly insulating nature of most MOFs. However, recent studies have demonstrated increasing interest in these composites for electromechanical applications [49]. This emerging focus is driven by the unique features of MOFs, which not only enhance the mechanical strength of hydrogels but also impart multifunctional properties such as adhesion, self-healing ability, and improved sensing capabilities. In the following subsections, recent advances in MOF–hydrogel composites for electromechanical sensing are reviewed, with particular emphasis on their use in strain sensors and triboelectric devices.

3.3.1 | *MOF–Hydrogel-Based Strain Sensor*

Strain sensors transduce external mechanical stimuli such as stretching or deformation into measurable electrical signals, typically observed as changes in resistance, capacitance, or voltage [192, 193]. Their performance depends on how effectively the material structure responds to mechanical input and converts it into an electrical output. Among various electromechanical sensors, strain sensors have been the most widely reported using MOF–hydrogel composites, owing to the inherent flexibility and stretchability of hydrogels. In a recent study, Rahman et al. [194] developed a ZIF-8-based MOF nanocomposite hydrogel using PAM and hydroxyethyl acrylate (HEA) through a one-pot synthesis method for strain sensing applications. The study highlighted the synergistic electrostatic interactions between the PAM–HEA polymer chains and the nanoporous ZIF-8, which significantly enhanced the mechanical properties of the hydrogel. In addition, abundant hydrogen bonds from the polarized surface of ZIF-8 imparted multifunctional features, such as self-healing, anti-freezing capability, and strong adhesion to various substrates, as demonstrated in Figure 6A [194]. By tuning the ZIF-8 content, the hydrogel achieved outstanding properties such as excellent stretchability (808%), high toughness (453.5 kJ/m^3), and minimal hysteresis (as low as 2.6%). The resulting strain sensor also exhibited strong adhesion, repeatable self-healing, resilience at −20°C, and high sensitivity with a gauge factor (GF) of 2.98 across a broad range, along with rapid response and recovery times of 280 and 330 ms, respectively (Figure 6A). In another study, Nimra et al. [116] created a supramolecular hydrogel composite by integrating Co-manganese MOFs (Co-Mn-MOFs) into a poly (lauryl methacrylate-acrylamide) network. To prevent MOF aggregation, the team used cetyltrimethylammonium bromide, a cationic surfactant, enabling uniform dispersion. This strategy led to synergistic reinforcement through hydrophobic and supramolecular interactions, yielding a hydrogel with remarkable mechanical properties, including ultra-stretchability (1655%), high toughness (447 kJ/m^3), and excellent anti-fatigue resistance (Figure 6B) [116] and a conductivity of 0.33 S/m. The strain sensor offered a wide detection range of 0.5%–700%, and a GF of 9.47 and ultrafast response/recovery times of 100 ms and 80 ms (Figure 6B). Other studies have likewise demonstrated the role of MOFs in enhancing the overall functional properties and sensitivity of hydrogels for strain sensing applications, as summarized in Table 5 [92, 96, 99, 114, 116, 118, 119, 194–200].

3.3.2 | *MOF–Hydrogel-Based TENG*

TENGs are a class of electromechanical sensors, often described as self-powered devices, since they can harvest energy from their surroundings. Their operation relies on triboelectrification (contact electrification), whereby electrical charges are transferred between two materials with differing electron affinities during repeated contact and separation [201–203]. Sliding, pressing, or vibrating motions generate electrostatic charges on the material surfaces, producing a potential difference that can be harnessed for sensing or energy harvesting.

Given this mechanism, MOFs have attracted growing interest for designing high-performance TENGs. Their tunable porosity and large surface areas provide abundant active sites for charge accumulation, while molecular-level tunability allows functionalization with electron-donating or withdrawing groups, thereby improving charge transfer efficiency [204–207]. Moreover, their molecular-level tunability enables the introduction of functional groups or metal centers with specific electron-donating or electron-withdrawing characteristics, improving charge transfer efficiency between triboelectric layers. MOFs can also enhance surface roughness and contact intimacy, leading to more effective charge generation. Their structural versatility also supports integration with various substrates, making them promising candidates for next-generation TENG-based energy harvesting and sensing systems. Furthermore, some MOFs exhibit intrinsic dielectric properties, enhancing capacitance and energy conversion efficiency.

Concomitantly, hydrogels offer unique advantages for TENG due to their flexibility, stretchability, and ionic conductivity [208–210]. Their soft, hydrated networks conform closely to triboelectric layers, improving contact and boosting triboelectrification efficiency. The high water content and tunable polymer networks within hydrogels facilitate ion migration and dynamic electrical double-layer formation, enhancing output performance. Hydrogels can also be engineered with tailored chemistries and mechanical properties to optimize triboelectric polarity and interface behavior. Their biocompatibility, transparency, and compatibility with diverse substrates make them excellent candidates for wearable, implantable, and environmentally adaptive TENG platforms. The chemical versatility of MOFs thus complements the mechanical and ionic advantages of hydrogels, enabling the development of flexible, lightweight, and multifunctional TENG devices. This hybrid approach overcomes the limitations of TENGs based solely on MOFs or hydrogels, offering enhanced performance through synergetic properties.

Rahman et al. [199] recently reported the development of a MOF-reinforced hydrogel electrode for wearable TENG by incorporating zeolitic imidazolate framework-8 (ZIF-8), a widely used MOF, into a PAM-co-hydroxyethyl acrylate hydrogel (Figure 7A) [199]. ZIF-8 nanocrystals acted as reinforcing nanofillers, enhancing the physical crosslinking of the hydrogel through numerous hydrogen bonds with the copolymer chains and improving stretchability and fatigue resistance of the hydrogel. LiCl was added to enhance ionic conductivity and impart anti-freezing properties. In this biphasic system, ZIF-8's cationic framework adsorbed Cl^- ions through electrostatic interactions, thereby increasing the local ionic concentration within the hydrogel matrix. This interaction

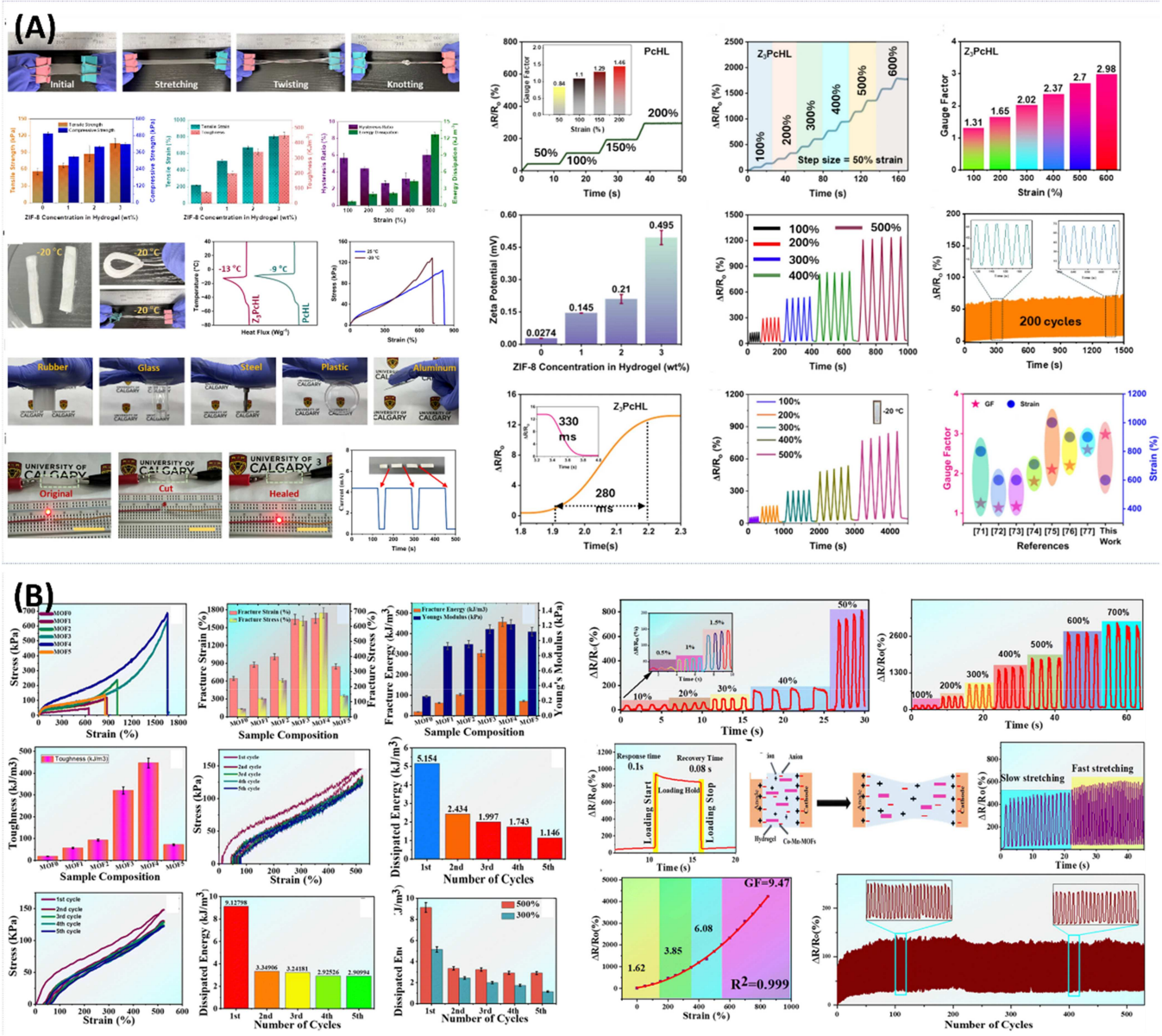

FIGURE 6 | (A) Demonstration of a ZIF-8-enhanced multifunctional nanocomposite hydrogel exhibiting excellent mechanical strength, stretchability, flexibility, toughness, strong adhesion, self-healing capability, and anti-freezing performance, enabling its application as a flexible and reliable strain sensor. Reproduced with permission: Copyright 2024, Springer Nature [194]. (B) Summary of the mechanical and strain-sensing performance of Co-Mn-MOFs reinforced hydrogel, demonstrating enhanced tensile strength, toughness, fatigue resistance, and stable, high sensitivity across both small and large strain ranges. Reproduced with permission: Copyright 2025, Royal Society of Chemistry [116].

plays a critical role in boosting the output performance of the ZIF-8 incorporated PAM-co-hydroxyethyl acrylate hydrogel. Under identical device configurations and input conditions, a TENG with 2 wt% ZIF-8 has achieved a maximum output voltage of 232 V and a current density of 56.3 mA/m^2, values around 1.8 times higher than those of the pure hydrogel-based device.

In a related study, Xu et al. [92] developed ZIF-8 nanoparticles as multifunctional crosslinkers within a PAM–polyvinylpyrrolidone double-network hydrogel (Figure 7B). Here, ZIF-8 acted as physical crosslinking sites, while NaCl introduced ionic conductivity. The resulting hydrogel displayed high flexibility, low mechanical hysteresis, and excellent electrical properties, making it a promising candidate for use as a flexible electrode in TENGs for efficient energy harvesting.

Although research into MOF–hydrogel-based TENG is still in its early stages, these findings demonstrate substantial potential. Continued work is needed to expand material design strategies and optimize device performance, as highlighted by the promising results summarized in Table 5.

4 | Advanced Applications of MOF–Hydrogel Nanocomposites-Based Sensors

As highlighted in the previous sections, MOF–hydrogel composites have been utilized in the development of various types of sensors, including optical, electrochemical, and electromechanical systems. By leveraging the synergistic properties of both MOFs and hydrogels, these composites offer high

TABLE 5 | Summary of MOF–hydrogel composites utilized in electromechanical sensors: sensing mechanisms, parameters, and performance metrics.

Composition	Sensor type	Sensing mechanism	Sensing parameter	Detected physical parameter	Detection range	Sensitivity	Response time (ms)	Ref.
PAA@UiO-66-NH_2	Strain	Piezoresistive due to ion mobility	Resistance	Stress & deformation	$\varepsilon = 800\%$	GF = 2.4	577	[118]
DMAA@Zr-MOF	Strain	Piezoresistive due to ion mobility	Resistance	Stress & deformation	$\varepsilon = 350\%$	GF = 10.12	—	[119]
Dodecyl methacrylate–PAM@BM-MOF	Strain	Piezoresistive due to ion mobility	Resistance	Stress & deformation	$\varepsilon = 700\%$	GF = 14.8	195–145	[96]
Dodecyl methacrylate–PAM@Zn-MOF	Strain	Piezoresistive due to ion mobility	Resistance	Stress, touch & pressure	$\varepsilon = 900\%$	GF = 6.5	80	[195]
PAM@MOF-525	Strain	Piezoresistive due to ion mobility	Resistance	Stress & deformation	$\varepsilon = 300\%$	GF = 1.38	—	[114]
Lauryl methacrylate-PAM@Co-Mn-MOF	Strain	Piezoresistive due to ion mobility	Resistance	Stress & deformation	$\varepsilon = 700\%$	GF = 9.47	100	[116]
PAM–PVP@ZIF-8	Strain	Piezoresistive due to ion mobility	Resistance	Stress & deformation	$\varepsilon = 1000\%$	GF = 6.38	140	[92]
PAM–HEA@ZIF-8	Strain	Piezoresistive due to ion mobility	Resistance	Stress & deformation	$\varepsilon = 600\%$	GF = 2.98	280	[194]
PAA@MXene/Fe-MIL-88NH_2	Strain	Piezoresistive due to electron conductivity	Resistance	Stress & deformation	$\varepsilon = 1000\%$	GF = 9.54	360	[99]
PVA–sodium carboxymethyl cellulose@rGO-CMOF	Strain	Piezoresistive due to electron conductivity	Resistance	Stress & deformation	$\varepsilon = 300\%$	GF = 0.41	40	[196]
PAM–PEGDA@MXene- HKUST-1/Fe_3O_4	Strain	Piezoresistive due to electron conductivity	Resistance	Stress & deformation	$\varepsilon = 600\%$	GF = 3.24	—	[197]
PAM–HEA@ZIF-67	Pressure	Electric double layer modulation	Capacitance	Stress, force & deformation	$P = 56$ kPa	0.75 kPa^{-1}	52.7	[198]
PVA–sodium carboxymethyl cellulose@rGO-CMOF	TENG	Contact electrification	Voltage	Force	1–5 Hz	$\rho = 1.89$ W/m^2	—	[196]
PAM–HEA@ZIF-8	TENG	Contact electrification & electrostatic induction	Voltage	Force	0.5–40 N	$\rho = 3.47$ W/m^2	—	[199]
PAM–PVP@ZIF-8	TENG	Contact electrification	Voltage	Force	0.5–3 Hz	$\rho = 0.34$ W/m^2	20	[92]
PVA–sodium carboxymethyl cellulose@2D Co-MOF	TENG	Contact electrification	Voltage	Force	—	$\rho = 2$ W/m^2	12	[200]

Abbreviations: ε = applied strain, ρ = power density, P = applied pressure.

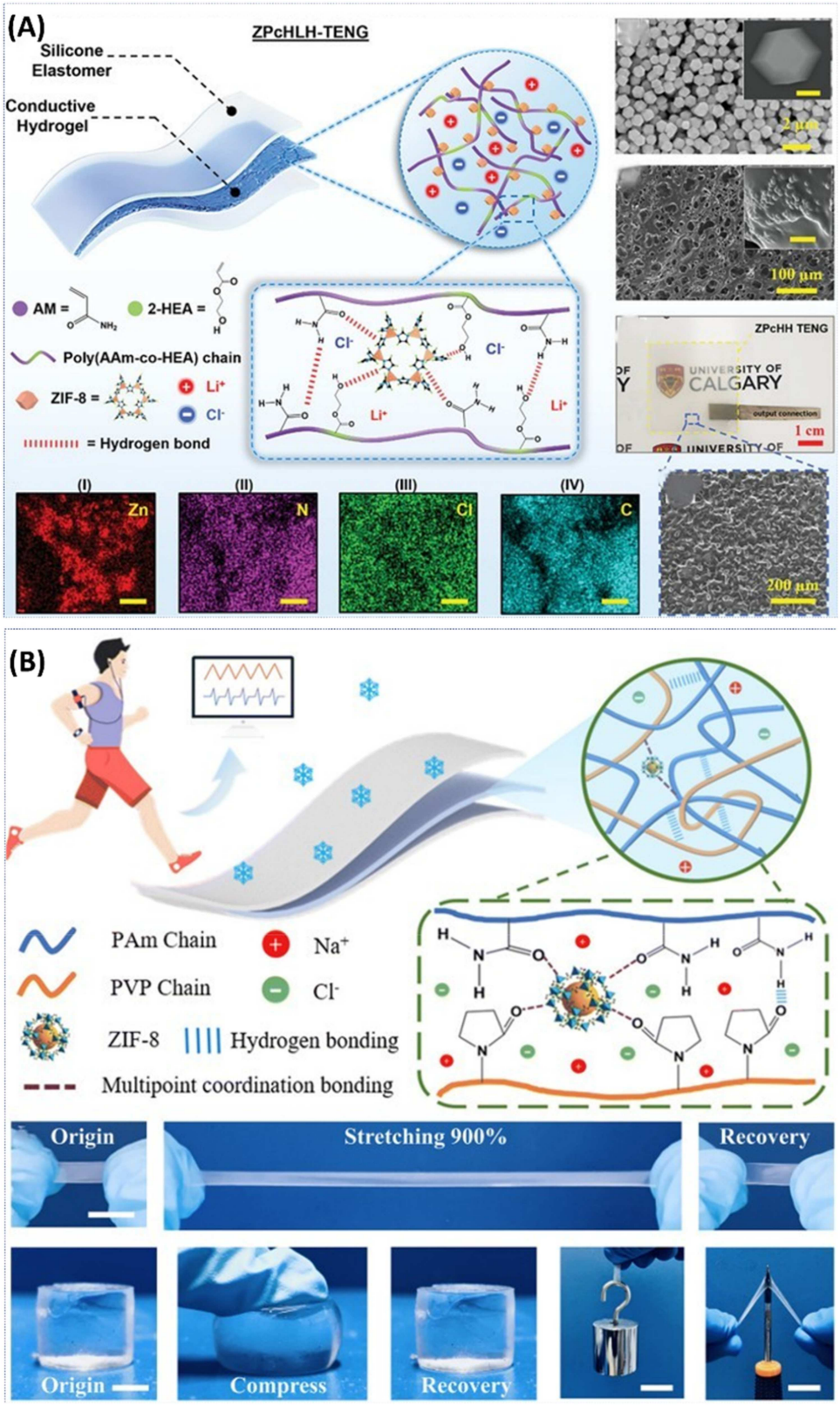

FIGURE 7 | (A) Schematic illustration of the ZIF-8@PAM-co-HEA with LiCl hydrogel-based TENG, along with the chemical structures and cross-linking networks of the nanocomposite hydrogel. Reproduced with permission: Copyright 2024, Wiley [199]. (B) ZIF-8 reinforced PAM/polyvinylpyrrolidone (PVP) flexible and stretchable hydrogel utilized in a TENG device as a self-powered sensor. Reproduced with permission: Copyright 2024, Royal Society of Chemistry [92].

sensitivity, multifunctionality, and adaptability, making them suitable for a wide range of sensing applications. In this section, we focus specifically on the application domains of these sensors. Based on the information summarized in Table 1, the applications have been categorized into healthcare and biomedical diagnostics, environmental monitoring, food safety and public health, flexible and wearable electronics, and human-computer and machine interaction technologies.

4.1 | Healthcare and Biomedical Diagnostics

The development of flexible healthcare sensing systems relies heavily on advanced materials with tailored functional, mechanical, and electrical properties. Among these, MOF–hydrogel composite-based sensors have emerged as highly promising candidates for healthcare and biomedical diagnostics due to their unique integration of functionality, biocompatibility, and mechanical adaptability. The incorporation of MOFs into hydrogels enabled the design of soft, flexible sensors with dynamic responsiveness to physiological stimuli, creating innovative platforms for personalized health management. Biocompatible, conductive nanocomposite hydrogels serve as key building blocks in soft, flexible sensor systems, offering dynamic responsiveness to physiological stimuli. By engineering MOFs surface chemistry or introducing specific functional groups, sensor selectivity can be precisely tailored to detect targeted analytes or biomarkers. MOFs can selectively capture biomolecules for disease monitoring or recognize volatile organic compounds indicative of pathological states. When embedded into hydrogel matrices, these functionalized MOFs yield unobtrusive, highly sensitive sensors suitable for real-time physiological monitoring and disease diagnostics. Figure 8 illustrates representative MOF–hydrogel-based sensors across optical (Figure 8A–C) [74, 79, 80], electrochemical (Figure 8D) [107], and electromechanical (Figure 8E,F) [194, 198] domains, emphasizing their applications in healthcare and biomedical diagnostics.

Several optical platforms highlight this potential. A Zn-MOF embedded SA hydrogel, doped with Eu^{3+}, enabled a pH-responsive luminescent film for dual detection of amino acids (aspartic acid and arginine), demonstrating its potential for real-time monitoring of biochemical markers in bodily fluids [82]. Another dual-readout biosensor was designed using hyaluronic acid (HAA) hydrogel integrated with aptamer-functionalized UiO-67-NH_2 MOFs via a viscosity-based flow sensor and fluorescence-based detection of Mucin 1, a biomarker linked to cancer [93]. Pyrene-based MOFs incorporated into hydrogels facilitated a robust pH-responsive fluorescence platform for detecting cardiac troponin I, relevant for early myocardial infarction diagnosis [124]. In cardiovascular diagnostics, MOF-525 nanosheets embedded in magnetic SA hydrogels allowed ultrasensitive thrombin detection, aided by magnetic separation and signal amplification [94].

For therapeutic drug monitoring, several MOF–hydrogels were developed. Among them, a MOF–hydrogel composite integrated with a smartphone readout platform enabled point-of-care isoniazid detection in urine and serum [74]. A nanocomposite hydrogel sensor utilizing MOF and SA was developed to identify β-lactamase in serum, relevant for penicillin allergy diagnostics [102]. A tetranuclear Eu-MOF combined with carbon dots and immobilized in a PAM hydrogel demonstrated ratiometric fluorescence sensing of phenylglyoxylic acid, an environmental exposure biomarker [167]. Another Eu-based MOF–hydrogel sensor was designed for the selective detection of hydroxyindole-3-acetic acid, a carcinoid tumor biomarker, integrated with smartphone imaging for real-time, point-of-care cancer diagnostics [80]. Glucose monitoring was advanced by embedding defective MOFs with immobilized enzymes in hydrogel matrices, significantly enhancing enzyme stability and enabling smartphone-assisted real-time diabetes management [107]. Multifunctional gelatin-based hydrogels encapsulating mixed-ligand MOFs and carbon dots demonstrated dual sensing and therapeutic capabilities with pH-responsive fluorescence for monitoring and wound healing promotion [108].

Other innovations extended MOF–hydrogel composites to wearable and implantable systems. Cu-hemin MOF–hydrogel biosensors enabled noninvasive glucose detection, while MOF–hydrogel microneedle arrays facilitated real-time cortisol monitoring, advancing stress diagnostics through skin-compatible wearable platforms [77]. A zirconium-based MOF integrated into photo-crosslinked hydrogels enabled free bilirubin detection in urine, useful for early liver dysfunction screening [161]. Lanthanide MOF–hydrogel composites served as ratiometric sensors for phosphate in human serum, supporting renal function diagnostics [87]. A corn-inspired microneedle array embedded with plasmonic MOFs allowed label-free SERS detection of acetaminophen, facilitating rapid and noninvasive drug monitoring [165].

Wearable electrochemical sensors further broaden applications. Fe/Co MOFs embedded in CS–PVA hydrogels enabled sweat-based lactic acid detection, while Ni-Co MOF–hydrogel smart contact lenses measured urea in tears, both with strong potential in personalized metabolic and physiological monitoring [73, 111]. For neurological and stress-related applications, Co-Ni MOFs embedded in CS–PAM hydrogels enabled adrenaline sensing with high electrocatalytic activity [181]. ZnS/MnO_2 MOF–hydrogel composites facilitated sensitive detection of glutathione in serum, highlighting their clinical relevance [186]. Core-shell MOF/COF composites in supramolecular hydrogels enabled portable electrochemical sensing of noradrenaline bitartrate [182]. Additionally, Co-MOF and vanadium carbide MXene hybrid hydrogel simultaneously detected levothyroxine and carbamazepine in serum, showing potential in point-of-care therapeutic drug monitoring [109].

4.2 | Environmental Monitoring, Food Safety, and Public Safety

With growing concerns over environmental pollution, foodborne illnesses, and public safety risks, the demand for sensitive, rapid, and cost-effective sensing platforms has intensified. MOF–hydrogel composite-based sensors have emerged as powerful tools for addressing challenges related to environmental contamination, food quality control, and public safety. Their combined properties, including the high surface area and chemical selectivity of MOFs along with the flexibility, responsiveness, and moisture retention capabilities of hydrogels, enable the detection of a wide range of hazardous

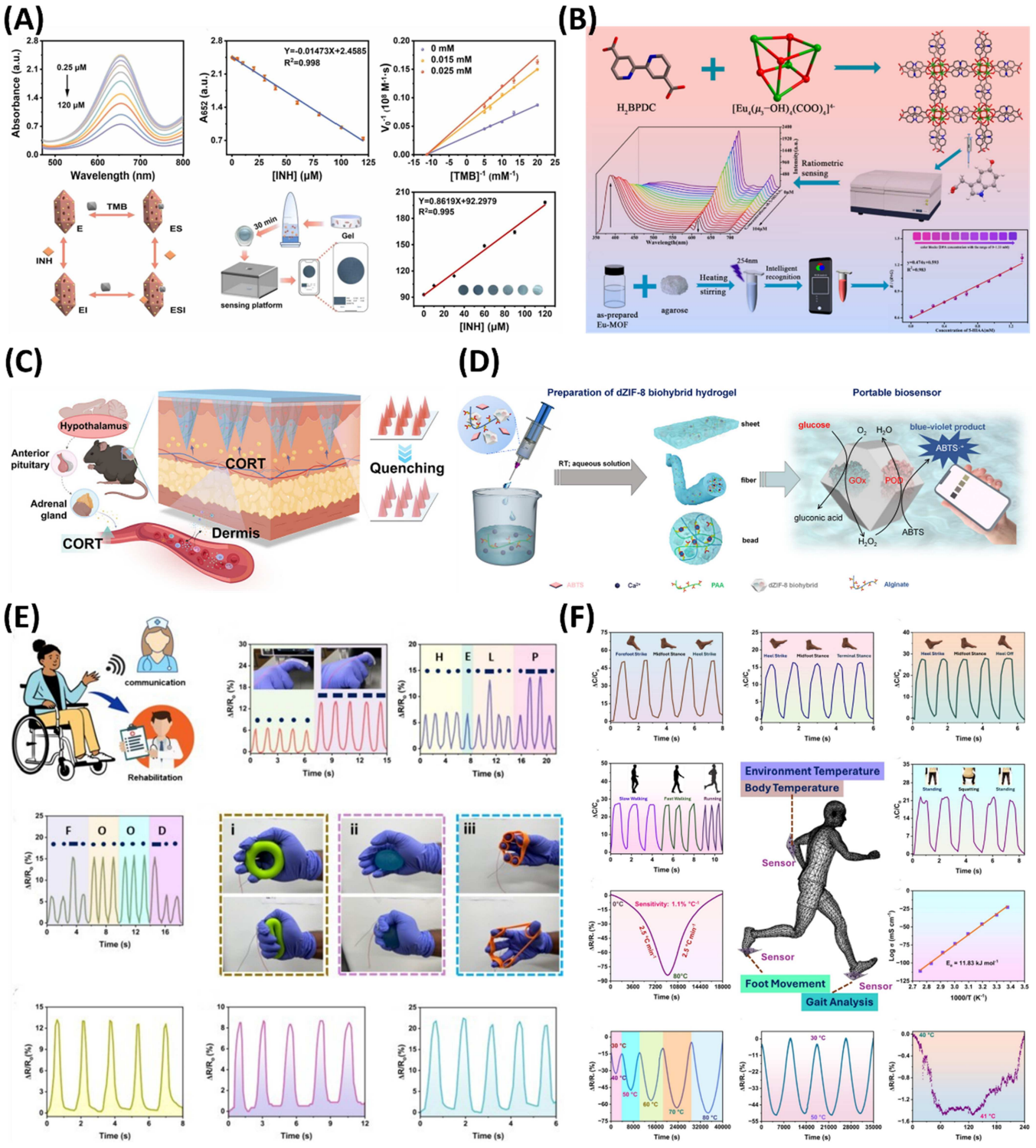

FIGURE 8 | Representative examples of MOF–hydrogel-based sensors for applications in healthcare and biomedical diagnostics. (A) A colorimetric sensing platform with integrated smartphone, based on a hydrogel matrix, constructed for the detection of isoniazid in urine and serum samples, with a focus on tuberculosis treatment. Reproduced with permission: Copyright 2023, Elsevier [74]. (B) Lanthanide MOF–hydrogel-based ratiometric photoluminescence sensor for on-site visual detection of the carcinoid biomarker 5 hydroxyindole 3 acetic acid. Reproduced with permission: Copyright 2024, American Chemical Society [80]. (C) Eu-MOF embedded in PEGDA and alginate hydrogel as a wearable sensor for visual monitoring of cortisol, applicable to conditions such as sleep disorders, depression, and chronic fatigue. Reproduced with permission: Copyright 2024, American Chemical Society [79]. (D) Encapsulation of enzymes into a defective MOF within a double crosslinked alginate hydrogel for a miniaturized portable glucose biosensor, enabling smartphone-assisted colorimetric detection of glucose. Reproduced with permission: Copyright 2022, American Chemical Society [107]. (E) ZIF-8 enhanced hydrogel-based strain sensors for rehabilitation training and improved patient-caregiver interactions. Reproduced with permission: Copyright 2024, Springer Nature [194]. (F) ZIF-67 incorporated organohydrogel-based capacitive pressure and temperature sensors for gait analysis and fever monitoring, offering potential applications in healthcare and sports science. Reproduced with permission: Copyright 2025, Elsevier [198].

substances. These include toxic gases, heavy metals, pesticide residues, and spoilage-related volatile compounds. In food systems, MOF–hydrogel sensors allow real-time monitoring of freshness and microbial contamination, supporting opportunities for intelligent packaging and spoilage prevention. In public safety contexts, such as air quality surveillance and detection of surface contamination in shared environments, these materials support rapid and portable sensing solutions.

Among the various sensing modes, optical and electrochemical MOF–hydrogel platforms are most frequently applied to environmental, food safety, and public safety monitoring. For example, a self-propelled fluorescence sensor was created by integrating ZIF-8 and Fe_3O_4 nanoparticles into a poly(acrylic acid-co-acrylamide) hydrogel, enabling both detection and removal of uranium from water, addressing nuclear waste risks [211]. A Eu-MOF-hydrogel bioreactor with programmable DNA probes was engineered for smart and portable fluorescence detection of heavy metal ions in water, offering real-time environmental surveillance [86]. UiO-66-NH_2 MOF embedded in agarose hydrogels enabled the detection of diethyl chlorophosphate vapor (a chemical warfare simulant), contributing to public safety through portable air monitoring [81]. A flexible gas sensor incorporating Fe-Co MOF within a PVA hydrogel was developed to detect acetone vapors at room temperature, aiming to monitor air quality in enclosed and industrial environments [110].

In food safety applications, MOF–hydrogel sensors have been employed for detecting spoilage markers, antibiotic residues, harmful additives, and antioxidant capacity. A dual-emission fluorescence sensor combining $Ru(bpy)_3^{2+}$ and UiO-OH MOF in a smart hydrogel was tailored for visual detection of trimethylamine in seafood [83]. A ratiometric fluorescence nanosensor encapsulating Rhodamine 6 G within an amino-functionalized UiO-66 MOF in gelatin hydrogel detected nitrite in meat products [88]. A portable Cu-MOF/SA hydrogel SERS platform selectively detected putrescine, a spoilage-related biogenic amine, in salmon and seawater [125].

Antibiotic detection has also advanced with MOF–hydrogel composites. Smartphone-compatible optical sensors using Fe/Zr bimetallic MOFs detected kanamycin and oxytetracycline, while a ratiometric fluorescence sensor integrating Eu^{3+}/carbon-dot modified MOF into a gelatin hydrogel for quantifying ofloxacin and tetracycline [78]. Other examples include a MOF-hybrid embedded in a nucleic-acid-based hydrogel for colorimetric detection of sarafloxacin, while a Eu-functionalized porphyrin-based MOF hydrogel for detection of sulfonamides in pork and milk, and an enoxacin-loaded Eu-MOF hydrogel integrated into paper and skin-attached devices for glyphosate detection [76, 106].

For broader food quality evaluation, MOF–hydrogel composites have also been used to measure total antioxidant capacity (TAC) and detect Cu^{2+} contamination and sense Fe^{3+} in water with long-term stability and reusability [105, 126]. Additionally, a Ce/Zr-MOF hydrogel with dual catalytic pathways was integrated into a wearable hydrogel patch for visual colorimetric sensing, enhancing on-site public safety [122].

Electrochemical sensors were also explored using MOF–hydrogel composites. A MOF-derived material in a nitrogen-doped graphene hydrogel enabled sensitive and selective detection of trolox in complex samples, demonstrating versatility across food, environmental, and biological contexts [85]. In addition, MOF–hydrogel beads fabricated by growing HKUST-1 in alginate and loading tea tree essential oil demonstrated antimicrobial action in fruit preservation, particularly for fresh-cut pineapple, offering an environmentally friendly strategy for food spoilage prevention through controlled release [137].

Figure 9A–E [85, 86, 105, 106, 211] highlights representative MOF–hydrogel-based sensors for environmental food safety and public safety applications, demonstrating their versatility in addressing real-world analytical challenges. Together, these advances demonstrate the versatility and efficacy of MOF–hydrogel composite sensors across a spectrum of real-world scenarios, including the detection of environmental contaminants, food spoilage, chemical threats, and harmful additives. Their integration with smartphones, different substrates, and wearable formats highlights their potential for point-of-use diagnostics in both resource-limited and advanced settings.

4.3 | Flexible and Wearable Electronics and Human–Machine Interface

MOF–hydrogel composites have recently emerged as promising materials for next-generation flexible and wearable electronics, as well as HMI technologies. Hydrogels have been extensively explored in these areas due to their tunable conductivity, mechanical flexibility, softness, and skin-like properties. By integrating the structural and functional advantages of MOFs with the stretchability and adaptability of hydrogels, these advanced hybrid materials enable the development of advanced sensing platforms with multifunctional capabilities. Their ability to adhere to diverse substrates, recover from deformation, and operate under repeated mechanical stress makes them robust platforms for long-term, real-world use.

Recent studies show that MOF–hydrogel-based electromechanical sensors are being predominantly explored in these applications due to their reliable signal output, adaptability to complex geometries, and compatibility with emerging technologies such as wearable displays and interactive interfaces. These developments position MOF–hydrogel composites as key enablers in the growing field of flexible and interactive electronics.

As a representative example, a self-powered wearable keypad system was developed using an array of ZIF-8 MOF-reinforced hydrogel-based TENG sensors integrated with a signal conditioning unit, as schematically illustrated in Figure 10A, demonstrating its suitability for self-powered HMI [199]. Another study reported the development of bimetallic-MOF-based tunable conductive hydrogels with artificial epidermis-like properties. These hydrogels exhibited smooth and responsive interaction with mobile touchscreens without noticeable delay, underscoring their potential to mimic human skin functionality (Figure 10B) [96]. Such performance highlights their promise as artificial e-skin materials for next-generation flexible electronic sensors, contributing to the advancement of interactive and adaptive electronic devices. Furthermore, a cascade catalytic system combining MXene and Fe-MIL-88NH_2 MOF enabled rapid, energy-free gelation of highly stretchable, tough, and conductive hydrogels, designed for wearable

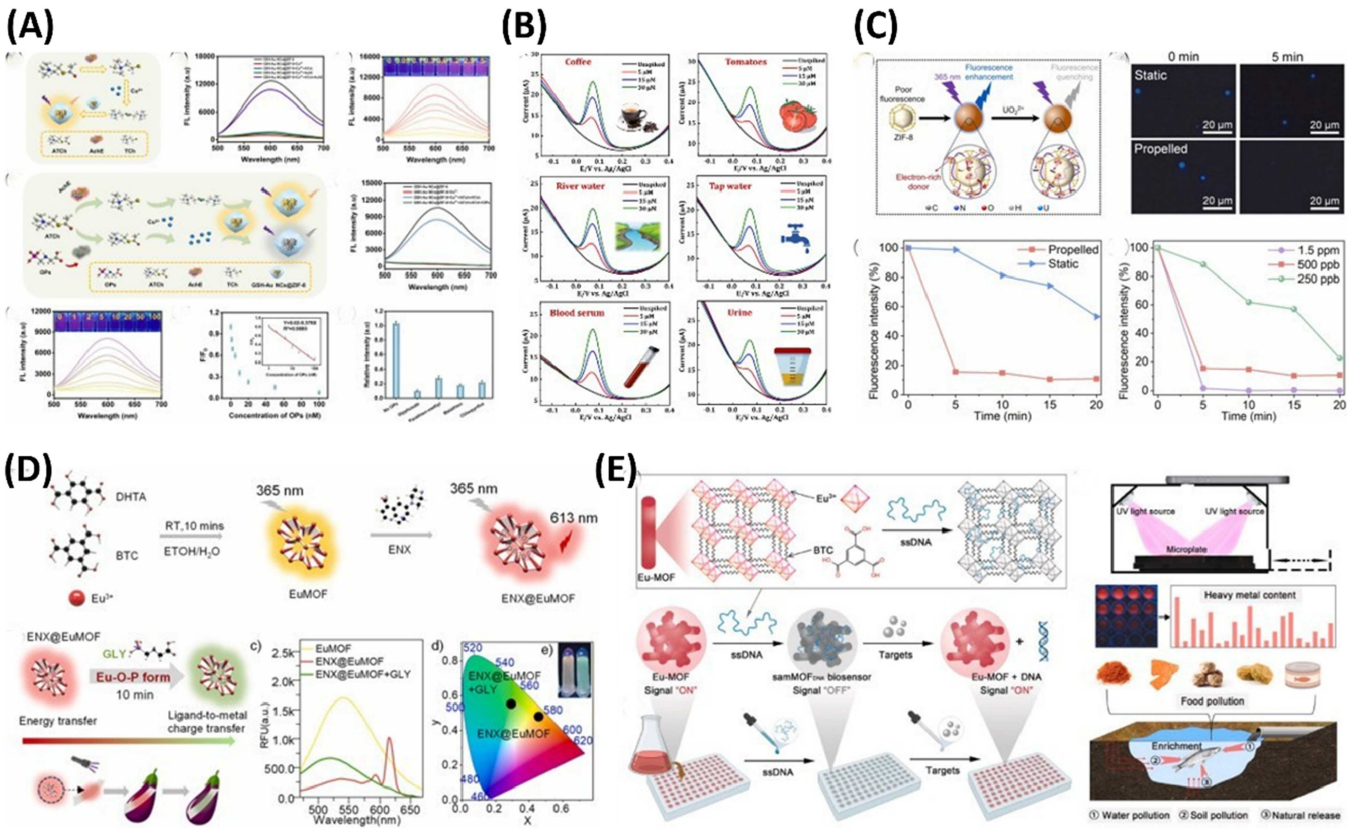

FIGURE 9 | Example of MOF–hydrogel-based sensors for applications in environmental monitoring, food safety, and public safety. (A) ZIF-8 MOF–hydrogel-based luminescent optical sensor for dual detection of acetylcholinesterase and organophosphates, highlighting its potential for contaminant monitoring. Reproduced with permission: Copyright 2023, Elsevier [105]. (B) MOF-derived nitrogen-doped graphene hydrogel-based electrochemical sensor for the sensitive detection of antioxidant Trolox in food, environmental, and biological samples. Reproduced with permission: Copyright 2024, Elsevier [85]. (C) Magnetically actuated ZIF-8 hydrogel composite micromotor-based fluorescence sensor for uranium detection, demonstrating fluorescence quenching with increasing uranium concentrations and enhanced performance for radioactive wastewater remediation. Reproduced with permission: Copyright 2024, Elsevier [211]. (D) Eu-MOF–hydrogel ratiometric sensors for applications in food safety, environmental, and agricultural monitoring, demonstrating glyphosate detection in contaminated food samples, including corn, sunflower seed, soybean, eggplant, citrus, and tea. Reproduced with permission: Copyright 2025, Elsevier [106]. (E) MOF-integrated hydrogel bioreactor for on-site detection of heavy metal ions, incorporating target recognition and smartphone-based imaging for portable environmental monitoring. Reproduced with permission: Copyright 2025, Elsevier [86].

electronics due to their exceptional mechanical and electrical performance [99]. In addition, mechano-responsive MOF–hydrogel-based sensors have been developed for handwriting recognition, capable of tracking and distinguishing different words written on their surfaces. These sensors function as handwriting sensors, accurately capturing and transmitting encrypted information, which offers significant potential for secure communication (Figure 10C) [92, 116, 200]. Notably, wearable systems of this type can transmit distress signals in emergencies, serving as vital tools for individuals with limited mobility or communication abilities.

Together, these developments highlight the high sensitivity, responsiveness, and multifunctionality of MOF–hydrogel composites, making them promising candidates for advanced HMIs and assistive technologies.

5 | Challenges and Future Perspectives

Building on the advances surveyed here, several priorities must be addressed for MOF–hydrogel sensors to move from laboratory prototypes to reliable devices across health, environmental monitoring, food safety, and public health. A comparative overview of advantages, disadvantages, challenges, and future perspectives for optical, electrochemical, and electromechanical platforms is provided in Table 6 and can serve as a practical checklist for study design and translation.

A key challenge is the integration and dispersion of MOFs within hydrogel precursors. While some studies report homogeneous dispersion under specific conditions, achieving uniformity remains difficult across pre-gel solutions of differing viscosities and rheological properties that depend on monomer type and solids content. In aqueous or low-viscosity media, slow or uneven gelation promotes aggregation, sedimentation, and spatial non-uniformity, which in turn lowers sensitivity and produces device-to-device variation. Beyond simple mixing, there is a need for pre-gel rheology control, compatibilizers that do not block pores or active sites, and in situ growth of MOFs within forming networks to improve interfacial bonding, spatial uniformity, and pore accessibility. Reporting standards should include quantitative analysis of MOF loading, dispersion maps

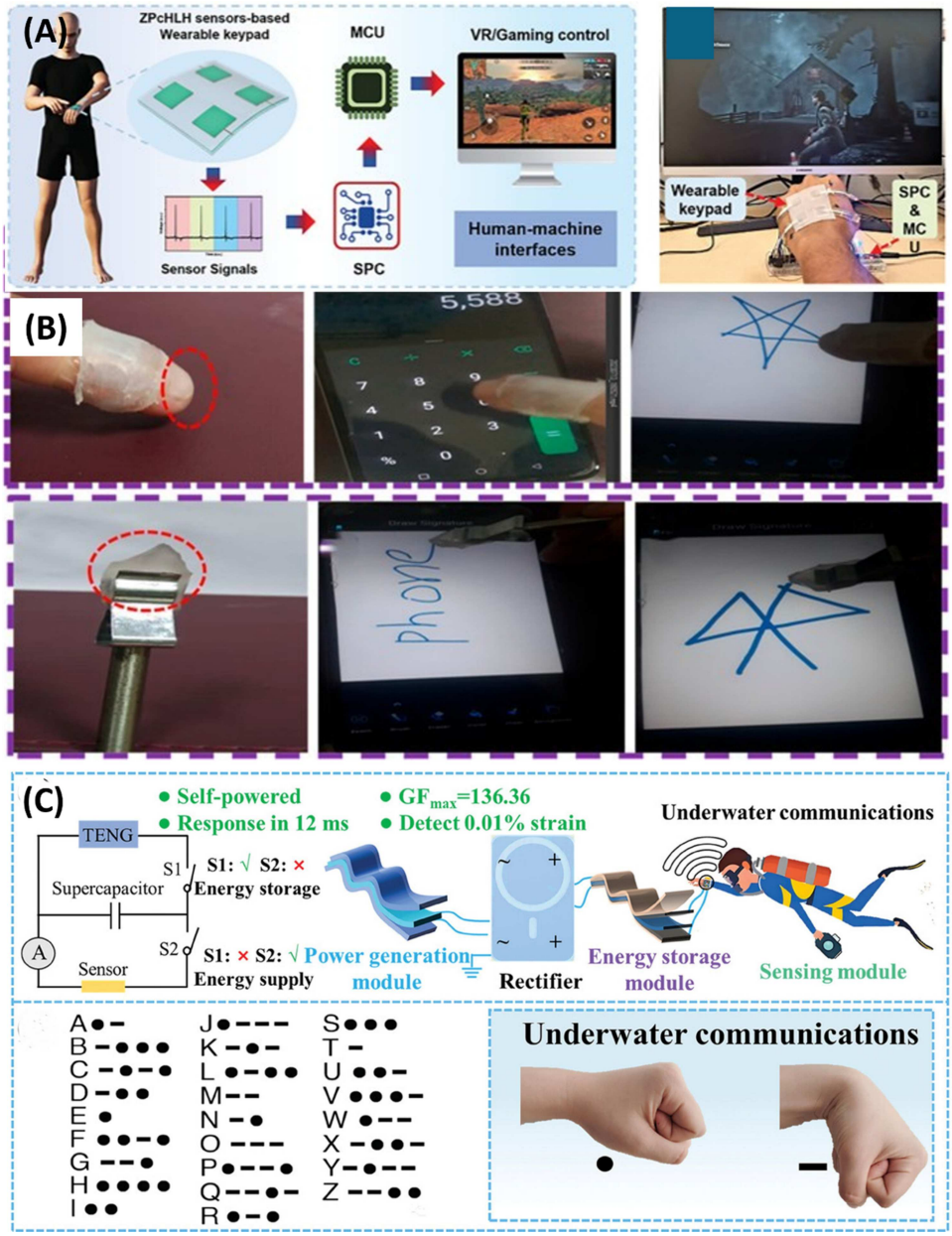

FIGURE 10 | Example of MOF–hydrogel-based sensors for applications in electronics and HMI. (A) System architecture of a ZIF-8 MOF-reinforced hydrogel-based TENG wearable keypad, demonstrating its application as an HMI for real-time interactive computer game control. Reproduced with permission: Copyright 2023, Wiley [199]. (B) Pressure-sensing behavior of the bimetallic MOF–hydrogel sensor used as a metallic pen for smart and touchscreens, demonstrating its potential in wearable electronic applications. Reproduced with permission: Copyright 2024, American Chemical Society [96]. (C) 2D conductive MOF–hydrogel-based self-powered TENG sensor for underwater communication, highlighting its application in wearable electronics for real-time signal transmission in aquatic environments. Reproduced with permission: Copyright 2025, Wiley [200].

across area or thickness, and pore accessibility checks by dye uptake or gas sorption after embedding.

Scalability and reproducibility remain bottlenecks. One-pot and mold casting routes are simple but rarely support high throughput or tight process control. Translation will require continuous mixing, slot die or blade coating, and roll-to-roll manufacturing with inline metrology for film thickness, swelling ratio, ionic conductivity, MOF loading proxies, and automated rejection of out-of-spec material. Lot traceability, statistical process control, and shared reporting of percent relative standard deviation for key metrics will reduce batch-to-batch variation. Additive manufacturing is promising for patterned and multiplexed devices but remains underused; printing windows should be defined in terms of ink viscosity, yield stress, and relaxation times, together with rules for avoiding sedimentation and sagging.

Geometry and mass transport are often under-optimized. Thickness, lateral dimensions, and microstructure strongly influence diffusion paths and response time. Thicker gels slow transport and increase lag, whereas thin films, fibers, microneedles, porous or microstructured surfaces, and microfluidic handling layers can shorten paths, stabilize sampling, and

TABLE 6 | Comparative overview of MOF–hydrogel sensors: advantages, disadvantages, challenges, and future perspectives.

Sensor type	Advantages	Disadvantages	Challenges	Future perspectives
Optical sensors	Dual emission; low background with high signal; enzyme-free workflow; visible colorimetric readout; long-lasting chemiluminescence without external light; nanoreactor confinement; portable real-time sensing; catalytic signal amplification; flexible handling; biocompatibility; low LOD	Photobleaching under UV; inner filter and self-absorption at higher analyte levels; intensity sensitive to illumination settings; interference from heavy metal ions and small molecules; limited reusability; non-linear kinetics complicate quantitation; possible MOF or dye leaching	Robust calibration across pH and ionic strength; long-term wet storage and handling; antifouling in complex matrices; spot-to-spot brightness uniformity; precise timing control for release steps; operation in complex samples without pretreatment; standardization of excitation and acquisition	Protective overcoat to reduce leaching; roll-to-roll fabrication of patterned arrays; ratiometric or lifetime encoded designs with internal reference; multi-analyte detection; smartphone readout and on-chip calibration; printable optical layers and microfluidic integration
Electrochemical sensors	Rapid response via fast analyte diffusion; mild aqueous processing; portable flexible form factor with conformal skin contact; compatible with food, environmental, and biological matrices; low voltage operation; enzyme-free operation; non-invasive sensing	MOF leaching; cross sensitivity to contaminants; contact resistance at interfaces; hydrogel dehydration over time; swelling-driven baseline drift; interference from coexisting matrix contaminants; oxidation or aging of conductive components	Selectivity in complex matrices; temperature and pH compensation; robust calibration across diverse matrices; strong adhesion to substrates or skin; on-body baseline stability; long-term stability and storage; reproducible MOF loading and uniform dispersion	Antifouling or permselective overcoat; MOF anchoring or encapsulation; continuous mixing and roll-to-roll scale-up; cross-platform validation and benchmarking; wireless readout and power integration; clinical validation; standardized electrode integration and inline QC; pathway to scalable printing or coating
Electromechanical sensors	Ultra-stretchable; wide strain window; high sensitivity; enhanced dielectric and mechanical strength; simple resistance voltage or capacitance readout; multifunctional sensing; recyclable device response; fast response and low power; conformal contact for human motion monitoring	Hysteresis and creep; transparency versus filler loading trade-off; contact resistance; charge dissipation in wet state; possible particle loss; temperature and humidity sensitivity	Long-term cycling durability; controlled rheology for uniform casting; reproducible particle size and surface chemistry; scalable mixing and casting; standardized strain calibration; robust adhesion and packaging; array-to-array uniformity; calibration in real motion and complex matrices; decoupling multimodal signals	Explore conductive MOFs; greener ionic liquids; breathable encapsulation for hydration control; wireless integration; data-driven drift correction; standardized testing and human subject validation; roll-to-roll patterning and printable electrodes; microstructure patterning to boost sensitivity

reduce matrix effects. Future studies need to emphasize quantifying characteristic diffusion lengths, response half-times, and the coupling between swelling state and signal.

Environmental robustness is another constraint. Hydrogels dehydrate at elevated temperatures and freeze at low temperatures, causing baseline drift in wearables and outdoor use. Organohydrogel formulations with benign cryo and humectant additives, together with breathable encapsulation that controls water loss while allowing vapor transport, can extend operating windows. Shelf life should be established through accelerated aging at elevated temperature and humidity with periodic checks of conductivity, modulus, and sensor baseline.

Electronic transduction presents additional challenges. Because most MOFs are not conductive, devices often rely on secondary fillers, introducing extra interfaces and contact resistance. Progress requires direct incorporation of conductive MOFs or mixed ionic electronic networks, careful preservation of pore accessibility and catalytic or optical function during polymerization, and engineered electrode interfaces or interlayers that lower resistance without blocking transport. Reporting should include contact resistance, percolation thresholds, and stability of electrical pathways under repeated strain and hydration cycles.

Adhesion and interfacial stability are critical in wearables. Hydrophilic matrices lose adhesion under perspiration and motion. Solutions include bioadhesive chemistries, topological interlocking, porous interlayers, and soft packaging to maintain conformal contact with skin, textiles, or device substrates. Practical metrics include wet/dry peel strength, water vapor transmission rate for comfort, and irritation testing on skin analogs or ex vivo tissue.

Safety and leachability need explicit evaluation, especially for on-body, food, or biomedical use. Strategies include covalent anchoring or in situ growth of MOFs inside networks, thin protective or permselective overcoats, and rigorous extractables and leachable testing alongside cytotoxicity and irritation assays. Metal release limits, residual monomer levels, and solvent residues should be quantified, and regeneration or end-of-life pathways should be considered to improve sustainability.

At the system level, effective sensing requires more than optimized material. Antifouling and permselective overcoats, low-power electronics, wireless telemetry, and on-device baseline correction must be integrated with robust calibration in complex matrices. For optical sensors, lifetime or wavelength encoded readouts reduce intensity drift; for colorimetric formats, standardized color cards and phone-to-phone calibration improve portability. For electrochemical devices, stable solid contact references, differential channels, and temperature and pH compensation are important. Data-driven methods and machine learning can support calibration transfer, drift compensation, and inference under variable conditions, but should be paired with transparent validation against reference methods.

Finally, standardization and benchmarking will accelerate progress. Community protocols for optical stability under ambient light, mechanical cycling to high cycle counts, humidity and temperature exposure, fouling resistance in relevant matrices, storage stability, and biocompatibility will enable fair comparisons across studies. Future research directions should focus on reporting a minimum set of performance metrics including limit of detection, linear range, response and recovery times, hysteresis, drift per hour under defined humidity and temperature, and operational lifetime under specified duty cycles.

Looking forward, the tunable surface chemistry, adjustable surface area and pore size, and diverse metal node configurations of MOFs, combined with the flexibility, biocompatibility, and tissue-like mechanics of hydrogels, define a co-design space for sensors that are selective, sensitive, and mechanically adaptive. Multifunctional features already demonstrated in MOF–hydrogel systems, including self-healing, adhesion, and freeze resistance, should be engineered deliberately to extend service life and enable stable operation in real environments. With coordinated advances in integration, scale-up, and quality control, environmental stability, electronic transduction, adhesion, safety, and system-level analytics, MOF–hydrogel platforms can become durable, reproducible, and integrable sensing systems for next-generation applications.

6 | Conclusion

This review comprehensively summarizes recent progress in MOF–hydrogel nanocomposite-based sensors and sensory systems, underscoring their broad potential across healthcare, environmental monitoring, food safety, and public health. We have outlined advances in optical, electrochemical, and electromechanical sensing, covering material chemistry, fabrication strategies, sensor architectures, performance parameters, and application landscapes. Integrating MOFs into hydrogel networks enhances mechanical strength, chemical stability, and thermal durability while imparting multifunctional properties such as self-healing, adhesion, and freeze resistance. The synergistic combination of tunable MOF chemistry and the flexibility and biocompatibility of hydrogels creates customizable, conformable, and highly integrable platforms ideal for advanced wearable and flexible electronics. Despite these advantages, real-world deployment remains constrained by challenges in uniform MOF dispersion, scalable manufacturing, environmental stability, and seamless integration of conductive and multifunctional architectures. Addressing these issues will require standardized characterization protocols, innovations in hybrid material chemistry, and advanced micro-nanofabrication methods. Looking ahead, coupling MOF–hydrogel sensors with wireless communication, self-powered operation, and AI-driven data analytics offers a pathway toward intelligent, autonomous, and adaptive sensing systems. With sustained interdisciplinary collaboration, these hybrid materials are poised to play a transformative role in next-generation high-performance, flexible, and application-adaptive sensing technologies.

Acknowledgments

This research was supported by the Tier 1 Canada Research Chair (CRC-2021-00489).

Conflicts of Interest

The authors declare no conflicts of interest.

Data Availability Statement

The authors have nothing to report.

References

1. A. M. Wright, M. T. Kapelewski, S. Marx, O. K. Farha, and W. Morris, "Transitioning Metal-Organic Frameworks From the Laboratory to Market Through Applied Research," *Nature Materials* 24, no. 2 (2024): 178–187.

2. H. C. Zhou, J. R. Long, and O. M. Yaghi, "Introduction to Metal-Organic Frameworks," *Chemical Reviews* 112, no. 2 (2012): 673–674.

3. H. Daglar and S. Keskin, "Recent Advances, Opportunities, and Challenges in High-Throughput Computational Screening of MOFs for Gas Separations," *Coordination Chemistry Reviews* 422 (2020): 213470.

4. M. Martos and I. M. Pastor, "Node Modification of Metal-Organic Frameworks for Catalytic Applications," *ChemistryOpen* 14, no. 7 (2025): e202400428.

5. C. Li, K. Wang, J. Li, and Q. Zhang, "Nanostructured Potassium-Organic Framework as an Effective Anode for Potassium-Ion Batteries With a Long Cycle Life," *Nanoscale* 12, no. 14 (2020): 7870–7874.

6. B. Srinivasan, A. Phani, X. Mu, K. Kim, S. Park, and S. Kim, "Tracking Molecular Signatures at ppb Sensitivity Using Fluctuational Kinetics in Metal-Organic Frameworks," *Nano Letters* 25, no. 19 (2025): 7924–7932.

7. R. P. S. Huynh, D. R. Evans, J. X. Lian, D. Spasyuk, S. Siahrostrami, and G. K. H. Shimizu, "Creating Order in Ultrastable Phosphonate Metal-Organic Frameworks via Isolable Hydrogen-Bonded Intermediates," *Journal of the American Chemical Society* 145, no. 39 (2023): 21263–21272.

8. Y. Wang, G. Yang, M. Chao, et al., "Molten Salts Etching Driven In-Situ Construction of MOF-Derived Co/Co-N-C/MXene Toward Oxygen Reduction Catalysis," *Energy & Fuels* 39, no. 17 (2025): 8283–8290.

9. R. R. Liang, Z. Liu, Z. Han, Y. Yang, J. Rushlow, and H. C. Zhou, "Anchoring Catalytic Metal Nodes Within a Single-Crystalline Pyrazolate Metal-Organic Framework for Efficient Heterogeneous Catalysis," *Angewandte Chemie International Edition* 64, no. 2 (2025): e202414271.

10. S. Lin, S. A. Kedzior, J. Zhang, et al., "A Superprotonic Membrane Derived From Proton-Conducting Metal-Organic Frameworks and Cellulose Nanocrystals," *Chem* 9, no. 9 (2023): 2547–2560.

11. Q. Li, M. Bai, X. Wang, et al., "A MOF@$ZnIn_2S_4$ Composite Quasi-Solid Electrolyte for Highly Reversible Zn-Ion Batteries," *Advanced Functional Materials* 35, no. 33 (2025): 2502344.

12. E. Kim, J. Lee, J. Park, H. Kim, and K. W. Nam, "Conductive MOF-Derived Coating for Suppressing the Mn Dissolution in $LiMn_2O_4$ Toward Long-Life Lithium-Ion Batteries," *Nano Letters* 25, no. 2 (2025): 619–627.

13. H. Wu, L. Wu, Y. Li, et al., "Direct Epitaxial Growth of Polycrystalline MOF Membranes on Cu Foils for Uniform Li Deposition in Long-Life Anode-Free Li Metal Batteries," *Angewandte Chemie International Edition* 64, no. 5 (2025): e202417209.

14. Z. Wang, T. Wu, L. Zeng, et al., "Machine Learning Relationships Between Nanoporous Structures and Electrochemical Performance in MOF Supercapacitors," *Advanced Materials* 37, no. 15 (2025): 2500943.

15. S. Wu, D. Cai, Z. Tian, L. Guo, and Y. Wang, "One-Step Synthesis of NiCo-MOF@LDH Hybrid Nanosheets for High-Performance Supercapacitor," *Journal of Energy Storage* 89 (2024): 111670.

16. B. Sarac, S. Yücer, and F. Ciftci, "MOF-Based Bioelectronic Supercapacitors," *Small* 21, no. 15 (2025): 2412846.

17. Y. Dong, J. Liu, H. Zhang, et al., "Novel Isostructural Iron-Series-MOF Calcined Derivatives as Positive and Negative Electrodes: A New Strategy to Obtain Matched Electrodes in a Supercapacitor Device," *SmartMat* 4, no. 3 (2023): e1159.

18. K. Wang, Z. Wang, J. Liu, et al., "Enhancing the Performance of a Battery-Supercapacitor Hybrid Energy Device Through Narrowing the Capacitance Difference Between Two Electrodes via the Utilization of 2D MOF-Nanosheet-Derived Ni@Nitrogen-Doped-Carbon Core-Shell Rings as Both Negative and Positive Electrodes," *ACS Applied Materials & Interfaces* 12, no. 42 (2020): 47482–47489.

19. S. Homayoonnia, A. Phani, and S. Kim, "MOF/MWCNT-Nanocomposite Manipulates High Selectivity to Gas via Different Adsorption Sites With Varying Electron Affinity: A Study in Methane Detection in Parts-Per-Billion," *ACS Sensors* 7, no. 12 (2022): 3846–3856.

20. W. L. Teo, J. Liu, W. Zhou, and Y. Zhao, "Facile Preparation of Antibacterial MOF-Fabric Systems for Functional Protective Wearables," *SmartMat* 2, no. 4 (2021): 567–578.

21. M. T. Khulood, U. S. Jijith, P. P. Naseef, S. M. Kallungal, V. S. Geetha, and K. Pramod, "Advances in Metal-Organic Framework-Based Drug Delivery Systems," *International Journal of Pharmaceutics* 673 (2025): 125380.

22. M. X. Wu and Y. W. Yang, "Metal–Organic Framework (MOF)-Based Drug/Cargo Delivery and Cancer Therapy," *Advanced Materials* 29, no. 23 (2017): 1606134.

23. Z. Guo, Y. Xiao, W. Wu, et al., "Metal–Organic Framework-Based Smart Stimuli-Responsive Drug Delivery Systems for Cancer Therapy: Advances, Challenges, and Future Perspectives," *Journal of Nanobiotechnology* 23, no. 1 (2025): 157.

24. L. Lu, L. Li, M. Chu, et al., "Recent Advancement in 2D Metal–Organic Framework for Environmental Remediation: A Review," *Advanced Functional Materials* 35, no. 14 (2025): 2419433.

25. R. Abazari, S. Sanati, W. K. Fan, et al., "Design and Engineering of MOF/LDH Hybrid Nanocomposites and LDHs Derived From MOF Templates for Electrochemical Energy Conversion/Storage and Environmental Remediation: Mechanism and Future Perspectives," *Coordination Chemistry Reviews* 523 (2025): 216256.

26. J. P. Gong, Y. Katsuyama, T. Kurokawa, and Y. Osada, "Double-Network Hydrogels With Extremely High Mechanical Strength," *Advanced Materials* 15, no. 14 (2003): 1155–1158.

27. Y. S. Zhang and A. Khademhosseini, "Advances in Engineering Hydrogels," *Science* 356, no. 6337 (2017): eaaf3627.

28. Y. Teng, J. Chi, J. Huang, et al., "Hydrogel Toughening Resets Biomedical Application Boundaries," *Progress in Polymer Science* 161 (2025): 101929.

29. N. R. Richbourg and N. A. Peppas, "The Swollen Polymer Network Hypothesis: Quantitative Models of Hydrogel Swelling, Stiffness, and Solute Transport," *Progress in Polymer Science* 105 (2020): 101243.

30. L. Hu, P. L. Chee, S. Sugiarto, et al., "Hydrogel-Based Flexible Electronics," *Advanced Materials* 35, no. 14 (2023): 2205326.

31. J. Ma, J. Zhong, F. Sun, et al., "Hydrogel Sensors for Biomedical Electronics," *Chemical Engineering Journal* 481 (2024): 148317.

32. X. Liu, J. Liu, S. Lin, and X. Zhao, "Hydrogel Machines," *Materials Today* 36 (2020): 102–124.

33. D. Zhang, Y. Tang, X. Gong, Y. Chang, and J. Zheng, "Highly Conductive and Tough Double-Network Hydrogels for Smart Electronics," *SmartMat* 5, no. 2 (2024): e1160.

34. Y. Chen, L. Chen, B. Geng, et al., "Triple-Network-Based Conductive Polymer Hydrogel for Soft and Elastic Bioelectronic Interfaces," *SmartMat* 5, no. 3 (2024): e1229.

35. Y. Chen, Y. Zhang, H. Li, et al., "Bioinspired Hydrogel Actuator for Soft Robotics: Opportunity and Challenges," *Nano Today* 49 (2023): 101764.

36. C. S. Park, Y. W. Kang, H. Na, and J. Y. Sun, "Hydrogels for Bioinspired Soft Robots," *Progress in Polymer Science* 150 (2024): 101791.

37. W. Zhang, P. Feng, J. Chen, Z. Sun, and B. Zhao, "Electrically Conductive Hydrogels for Flexible Energy Storage Systems," *Progress in Polymer Science* 88 (2019): 220–240.

38. C. Shen, Y. Han, H. Xiong, et al., "Multifunctional Hydrogel Scaffolds Based on Polysaccharides and Polymer Matrices Promote Bone Repair: A Review," *International Journal of Biological Macromolecules* 294 (2025): 139418.

39. H. Zhang, S. Wu, W. Chen, Y. Hu, Z. Geng, and J. Su, "Bone/Cartilage Targeted Hydrogel: Strategies and Applications," *Bioactive Materials* 23 (2023): 156–169.

40. H. Cao, L. Duan, Y. Zhang, J. Cao, and K. Zhang, "Current Hydrogel Advances in Physicochemical and Biological Response-Driven Biomedical Application Diversity," *Signal Transduction and Targeted Therapy* 6, no. 1 (2021): 426.

41. B. H. Shan and F. G. Wu, "Hydrogel-Based Growth Factor Delivery Platforms: Strategies and Recent Advances," *Advanced Materials* 36, no. 5 (2023): 2210707.

42. Y. Liu, J. Wang, H. Chen, and D. Cheng, "Environmentally Friendly Hydrogel: A Review of Classification, Preparation and Application in Agriculture," *Science of the Total Environment* 846 (2022): 157303.

43. M. A. S. Salem, A. S. Bhat, R. Mehandi, et al., "Advances in Sensing Technologies Using Functional Carbon Nanotube-Hydrogel Nanocomposites," *Inorganic Chemistry Communications* 175 (2025): 114139.

44. A. Alam, Y. Zhang, H. C. Kuan, S. H. Lee, and J. Ma, "Polymer Composite Hydrogels Containing Carbon Nanomaterials—Morphology and Mechanical and Functional Performance," *Progress in Polymer Science* 77 (2018): 1–18.

45. A. M. Gutierrez, E. M. Frazar, M. V. X. Klaus, P. Paul, and J. Z. Hilt, "Hydrogels and Hydrogel Nanocomposites: Enhancing Healthcare Through Human and Environmental Treatment," *Advanced Healthcare Materials* 11, no. 7 (2022): 2101820.

46. Y. Lin, A. Wu, Y. Zhang, H. Duan, P. Zhu, and Y. Mao, "Recent Progress of Nanomaterials-Based Composite Hydrogel Sensors for Human–Machine Interactions," *Discover Nano* 20, no. 1 (2025): 60.

47. X. Sun, F. Yao, and J. Li, "Nanocomposite Hydrogel-Based Strain and Pressure Sensors: A Review," *Journal of Materials Chemistry A* 8, no. 36 (2020): 18605–18623.

48. L. Wang, H. Xu, J. Gao, J. Yao, and Q. Zhang, "Recent Progress in Metal-Organic Frameworks-Based Hydrogels and Aerogels and Their Applications," *Coordination Chemistry Reviews* 398 (2019): 213016.

49. W. Sun, X. Zhao, E. Webb, G. Xu, W. Zhang, and Y. Wang, "Advances in Metal-Organic Framework-Based Hydrogel Materials: Preparation, Properties and Applications," *Journal of Materials Chemistry A* 11, no. 5 (2023): 2092–2127.

50. J. Y. C. Lim, L. Goh, K. Otake, S. S. Goh, X. J. Loh, and S. Kitagawa, "Biomedically-Relevant Metal Organic Framework-Hydrogel Composites," *Biomaterials Science* 11, no. 8 (2023): 2661–2677.

51. Z. Zhuang, Z. Mai, T. Wang, and D. Liu, "Strategies for Conversion Between Metal–Organic Frameworks and Gels," *Coordination Chemistry Reviews* 421 (2020): 213461.

52. H. Meskher, S. B. Belhaouari, and F. Sharifianjazi, "Mini Review About Metal Organic Framework (MOF)-Based Wearable Sensors: Challenges and Prospects," *Heliyon* 9, no. 11 (2023): e21621.

53. I. Stassen, N. Burtch, A. Talin, P. Falcaro, M. Allendorf, and R. Ameloot, "An Updated Roadmap for the Integration of Metal-Organic Frameworks With Electronic Devices and Chemical Sensors," *Chemical Society Reviews* 46, no. 11 (2017): 3185–3241.

54. W. Wu, Y. Li, P. Song, et al., "Metal-Organic Framework (MOF)-Based Sensors for Exogenous Contaminants in Food: Mechanisms, Advances, and Prospects," *Trends in Food Science & Technology* 138 (2023): 238–271.

55. X. Lu, K. Jayakumar, Y. Wen, A. Hojjati-Najafabadi, X. Duan, and J. Xu, "Recent Advances in Metal-Organic Framework (MOF)-Based Agricultural Sensors for Metal Ions: A Review," *Microchimica Acta* 191, no. 1 (2024): 58.

56. X. Xu, M. Ma, T. Sun, X. Zhao, and L. Zhang, "Luminescent Guests Encapsulated in Metal–Organic Frameworks for Portable Fluorescence Sensor and Visual Detection Applications: A Review," *Biosensors* 13, no. 4 (2023): 435.

57. H. Y. Li, S. N. Zhao, S. Q. Zang, and J. Li, "Functional Metal-Organic Frameworks as Effective Sensors of Gases and Volatile Compounds," *Chemical Society Reviews* 49, no. 17 (2020): 6364–6401.

58. X. Fang, B. Zong, and S. Mao, "Metal–Organic Framework-Based Sensors for Environmental Contaminant Sensing," *Nano-Micro Letters* 10, no. 4 (2018): 64.

59. C. H. Chuang and C. W. Kung, "Metal−Organic Frameworks Toward Electrochemical Sensors: Challenges and Opportunities," *Electroanalysis* 32, no. 9 (2020): 1885–1895.

60. M. Bosch, S. Yuan, W. Rutledge, and H. C. Zhou, "Stepwise Synthesis of Metal-Organic Frameworks," *Accounts of Chemical Research* 50, no. 4 (2017): 857–865.

61. N. Stock and S. Biswas, "Synthesis of Metal-Organic Frameworks (MOFs): Routes to Various MOF Topologies, Morphologies, and Composites," *Chemical Reviews* 112, no. 2 (2012): 933–969.

62. S. Yuan, L. Feng, K. Wang, et al., "Stable Metal–Organic Frameworks: Design, Synthesis, and Applications," *Advanced Materials* 30, no. 37 (2018): 1704303.

63. E. A. Flügel, A. Ranft, F. Haase, and B. V. Lotsch, "Synthetic Routes Toward MOF Nanomorphologies," *Journal of Materials Chemistry* 22 (2012): 10119–10133.

64. W. He, D. Lv, Y. Guan, and S. Yu, "Post-Synthesis Modification of Metal-Organic Frameworks: Synthesis, Characteristics, and Applications," *Journal of Materials Chemistry A* 11, no. 45 (2023): 24519–24550.

65. M. Safaei, M. M. Foroughi, N. Ebrahimpoor, S. Jahani, A. Omidi, and M. Khatami, "A Review on Metal-Organic Frameworks: Synthesis and Applications," *Trends in Analytical Chemistry* 118 (2019): 401–425.

66. X. Cai, Z. Xie, D. Li, M. Kassymova, S. Q. Zang, and H. L. Jiang, "Nano-Sized Metal-Organic Frameworks: Synthesis and Applications," *Coordination Chemistry Reviews* 417 (2020): 213366.

67. C. Liu, J. Wang, J. Wan, and C. Yu, "MOF-on-MOF Hybrids: Synthesis and Applications," *Coordination Chemistry Reviews* 432 (2021): 213743.

68. R. He, J. He, J. Shen, H. Fu, Y. Zhang, and B. Wang, "Recent Advances in Multifaceted Applications of MOF-Based Hydrogels," *Soft Science* 4, no. 4 (2024): 37.

69. P. Kush, R. Singh, and P. Kumar, "Recent Advances in Metal–Organic Framework-Based Anticancer Hydrogels," *Gels* 11, no. 1 (2025): 76.

70. Y. Liu, N. E. Vrana, P. A. Cahill, and G. B. McGuinness, "Physically Crosslinked Composite Hydrogels of PVA With Natural Macromolecules: Structure, Mechanical Properties, and Endothelial Cell Compatibility," *Journal of Biomedical Materials Research, Part B: Applied Biomaterials* 90B, no. 2 (2009): 492–502.

71. W. Hu, Z. Wang, Y. Xiao, S. Zhang, and J. Wang, "Advances in Crosslinking Strategies of Biomedical Hydrogels," *Biomaterials Science* 7, no. 3 (2019): 843–855.

72. M. M. Elsayed, "Hydrogel Preparation Technologies: Relevance Kinetics, Thermodynamics and Scaling Up Aspects," *Journal of Polymers and the Environment* 27, no. 4 (2019): 871–891.

73. G. Mukundan, M. Ravipati, and S. Badhulika, "Bimetallic Fe/Co-MOF Dispersed in a PVA/Chitosan Multi-Matrix Hydrogel as a Flexible Sensor for the Detection of Lactic Acid in Sweat Samples," *Microchimica Acta* 191, no. 10 (2024): 614.

74. J. Yu, Q. Sun, J. Sun, X. Wang, N. Niu, and L. Chen, "Development of Gold Nanoparticles Composite Functionalized Bimetallic Metal-

Organic Framework Nanozymes and Integrated Smartphone to Detection Isoniazid," *Sensors and Actuators B: Chemical* 390 (2023): 134024.

75. Y. Lu, M. Wei, C. Wang, W. Wei, and Y. Liu, "Enhancing Hydrogel-Based Long-Lasting Chemiluminescence by a Platinum-Metal Organic Framework and Its Application in Array Detection of Pesticides and D-Amino Acids," *Nanoscale* 12, no. 8 (2020): 4959–4967.

76. M. Jie, S. Lan, B. Zhu, et al., "Europium Functionalized Porphyrin-Based Metal-Organic Framework Heterostructure and Hydrogel for Visual Ratiometric Fluorescence Sensing of Sulfonamides in Foods," *Food Chemistry* 458 (2024): 140304.

77. C. Lin, Y. Du, S. Wang, L. Wang, and Y. Song, "Glucose Oxidase@Cu-Hemin Metal-Organic Framework for Colorimetric Analysis of Glucose," *Materials Science and Engineering: C* 118 (2021): 111511.

78. E. C. Aham, A. Ravikumar, K. Zeng, et al., "Intelligent Hydrogel and Smartphone-Assisted Colorimetric Sensor Based on Bi-Metallic Organic Frameworks for Effective Detection of Kanamycin and Oxytetracycline," *Microchimica Acta* 192, no. 3 (2025): 201.

79. K. Liu, H. Wang, F. Zhu, et al., "Lab on the Microneedles: A Wearable Metal-Organic Frameworks-Based Sensor for Visual Monitoring of Stress Hormone," *ACS Nano* 18, no. 22 (2024): 14207–14217.

80. E. Wang, L. Li, J. Y. Zou, et al., "Regulating the Energy Level of a Ratiometric Luminescent Europium(III) Metal-Organic Framework Sensor With Smartphone Assistance for Real-Time and Visual Detection of Carcinoid Biomarker," *Inorganic Chemistry* 64, no. 8 (2025): 3930–3940.

81. Y. Lei, Y. Gao, Y. Xiao, P. Huang, and F. Y. Wu, "Zirconium-Based Metal-Organic Framework Loaded Agarose Hydrogels for Fluorescence Turn-On Detection of Nerve Agent Simulant Vapor," *Analytical Methods* 15, no. 42 (2023): 5674–5682.

82. H. Sha and B. Yan, "A pH-Responsive Eu(III) Functionalized Metal-Organic Framework Hybrid Luminescent Film for Amino Acid Sensing and Anti-Counterfeiting," *Journal of Materials Chemistry C* 10, no. 19 (2022): 7633–7640.

83. P. Jia, X. He, J. Yang, et al., "Dual–Emission MOF–Based Ratiometric Platform and Sensory Hydrogel for Visible Detection of Biogenic Amines in Food Spoilage," *Sensors and Actuators B: Chemical* 374 (2023): 132803.

84. H. Jiang, S. Qi, X. Dong, B. Ang, Y. Zhang, and Z. Wang, "Integrating Metal-Organic Framework Hybrid into Nucleic Acid-Based Hydrogel for Highly Selective Recognition and Sensitive Detection of Sarafloxacin," *Analytical Chemistry* 97, no. 20 (2025): 10550–10560.

85. A. Ashokrao Jagtap, R. Sakthivel, S. Kubendhiran, et al., "Metal-Organic Framework Derived $Mn_{0.2}Zn_{0.8}Se$/C Amalgamated With Nitrogen-Doped Graphene Hydrogel for Antioxidant Trolox Detection in Food, Environmental, and Biological Samples," *Chemical Engineering Journal* 496 (2024): 154178.

86. X. Mao, M. Shi, C. Chen, et al., "Metal-Organic Framework Integrated Hydrogel Bioreactor for Smart Detection of Metal Ions," *Biosensors and Bioelectronics* 247 (2024): 115919.

87. N. Gao, J. Huang, L. Wang, J. Feng, P. Huang, and F. Wu, "Ratiometric Fluorescence Detection of Phosphate in Human Serum With a Metal-Organic Frameworks-Based Nanocomposite and Its Immobilized Agarose Hydrogels," *Applied Surface Science* 459 (2018): 686–692.

88. S. Deng, J. Liu, D. Han, et al., "Synchronous Fluorescence Detection of Nitrite in Meat Products Based on Dual-Emitting Dye@MOF and Its Portable Hydrogel Test Kit," *Journal of Hazardous Materials* 463 (2024): 132898.

89. L. Zhao, J. Gan, T. Xia, et al., "A Luminescent Metal-Organic Framework Integrated Hydrogel Optical Fibre as a Photoluminescence Sensing Platform for Fluorescence Detection," *Journal of Materials Chemistry C* 7, no. 4 (2019): 897–904.

90. Z. Lu, X. Liu, X. Zhu, et al., "Rational Design of Mixed-Ligand Metal–Organic Framework With Dual Emission Signals for Real-Time Visual Detection and Efficient Adsorption of Glyphosate in Water," *Journal of Hazardous Materials* 494 (2025): 138683.

91. G. Wang, Z. Liao, Z. Jiang, et al., "A MOF/Hydrogel Film-Based Array Sensor for Discriminative Detection of Nitrophenol Isomers," *Journal of Materials Chemistry C* 11, no. 42 (2023): 14551–14558.

92. J. Xu, J. Liang, J. Zheng, et al., "Zeolitic Imidazolate Framework-Enhanced Conductive Nanocomposite Hydrogels With High Stretchability and Low Hysteresis for Self-Powered Multifunctional Sensors," *Journal of Materials Chemistry A* 13, no. 17 (2025): 12256–12265.

93. Y. Wang, D. Zhang, Y. Zeng, Y. Sun, and P. Qi, "A Universal Dual-Readout Viscosity Flow Sensor Based on Biotarget-Triggered Hyaluronidase Release From Aptamer-Capped Metal-Organic Frameworks," *Sensors and Actuators B: Chemical* 372 (2022): 132637.

94. Y. Lin, Y. Sun, Y. Dai, et al., "A 'Signal-On' Chemiluminescence Biosensor for Thrombin Detection Based on DNA Functionalized Magnetic Sodium Alginate Hydrogel and Metalloporphyrinic Metal-Organic Framework Nanosheets," *Talanta* 207 (2020): 120300.

95. W. Tong, J. Liu, S. Liu, et al., "ZIF-8-Induced Fluorescence-Enhanced Multifunctional MOF-on-MOF Hydrogels for Efficient Adsorption and Sensitive Detection of Uranyl Ions in Water," *Talanta* 295 (2025): 128299.

96. M. Khan, L. A. Shah, P. Hifsa, H. M. Yoo, H. M. Yoo, and D. J. Kwon, "Bimetallic-MOF Tunable Conductive Hydrogels to Unleash High Stretchability and Sensitivity for Highly Responsive Flexible Sensors and Artificial Skin Applications," *ACS Applied Polymer Materials* 6, no. 12 (2024): 7288–7300.

97. J. Zhang, Y. Gao, L. Song, and H. Hong, "Ratiometric Fluorescent and Visual Detection of Arginine With a Dual-Ligand MOF–Based Sensing Platform," *Journal of Molecular Structure* 1328 (2025): 141321.

98. S. Javanbakht, M. Pooresmaeil, H. Hashemi, and H. Namazi, "Carboxymethylcellulose Capsulated Cu-Based Metal-Organic Framework-Drug Nanohybrid as a pH-Sensitive Nanocomposite for Ibuprofen Oral Delivery," *International Journal of Biological Macromolecules* 119 (2018): 588–596.

99. Y. Liu, X. Zou, B. Luo, Z. Li, L. Yu, and Y. Wu, "Cascaded MXene/Metal-Organic Framework System Enables Rapid Gelation of Ultrastretchable and High-Toughness Conductive Hydrogels for Multifunctional Wearable Electronics," *Chemical Engineering Journal* 503 (2025): 158288.

100. Y. Liu, X. Zhou, W. Zhu, et al., "Ce/Zr-MOF With Dual Cycle Synergistic Catalysis Pathway Enabling Enhanced Peroxidase-Like Performance for Wearable Hydrogel Patch Visualization Sensing Platform," *Inorganic Chemistry* 62, no. 37 (2023): 15022–15030.

101. K. Ren, Y. Li, and Q. Liu, "Rapid On-Site Colorimetric Detection of Arsenic(V) by NH_2-MIL-88(Fe) Nanozymes-Based Ultraviolet-Visible Spectroscopic and Smartphone-Assisted Sensing Platforms," *Analytica Chimica Acta* 1336 (2025): 343523.

102. X. Lian and B. Yan, "Diagnosis of Penicillin Allergy: A MOFs-Based Composite Hydrogel for Detecting β-Lactamase in Serum," *Chemical Communications* 55, no. 2 (2019): 241–244.

103. H. Sha and B. Yan, "Dye-Functionalized Metal-Organic Frameworks With the Uniform Dispersion of MnO_2 Nanosheets for Visualized Fluorescence Detection of Alanine Aminotransferase," *Nanoscale* 13, no. 47 (2021): 20205–20212.

104. X. Nie, X. Han, S. Yu, W. Liu, and Y. Yang, "Embedding Gold Nanoclusters in Metal-Organic Frameworks as a Dual-Channel Hydrogel Optical Sensor for Hydrogen Sulfide Detection," *Journal of Solid State Chemistry* 346 (2025): 125283.

105. D. Wei, M. Li, Y. Wang, et al., "Encapsulating Gold Nanoclusters Into Metal–Organic Frameworks to Boost Luminescence for Sensitive

Detection of Copper Ions and Organophosphorus Pesticides," *Journal of Hazardous Materials* 441 (2023): 129890.

106. L. Bai, Z. Li, Q. Liu, et al., "Enoxacin-Embedded EuMOF-Based Ratio Fluorescent Sensing Platform Integrated With Paper-Based Sensor and Skin-Attachable Hydrogel for Glyphosate Detection in Foods," *Journal of Hazardous Materials* 489 (2025): 137658.

107. N. Zhong, R. Gao, Y. Shen, et al., "Enzymes-Encapsulated Defective Metal-Organic Framework Hydrogel Coupling With a Smartphone for a Portable Glucose Biosensor," *Analytical Chemistry* 94, no. 41 (2022): 14385–14393.

108. S. K. Bhattacharyya, S. Nandi, T. Dey, et al., "Fabrication of a Vitamin B_{12}-Loaded Carbon Dot/Mixed-Ligand Metal Organic Framework Encapsulated Within the Gelatin Microsphere for pH Sensing and in Vitro Wound Healing Assessment," *ACS Applied Bio Materials* 5, no. 12 (2022): 5693–5705.

109. M. Ravipati, D. Ramasamy, and S. Badhulika, "Highly Selective Cobalt-MOF/Vanadium Carbide MXene Hydrogel for Simultaneous Electrochemical Determination of Levothyroxine and Carbamazepine in Simulated Blood Serum," *Electrochimica Acta* 525 (2025): 146154.

110. B. Maji, P. Singh, and S. Badhulika, "A Highly Sensitive and Fully Flexible Fe-Co Metal-Organic Framework Hydrogel Based Gas Sensor for ppb Level Detection of Acetone," *Applied Surface Science* 678 (2024): 161047.

111. G. Mukundan and S. Badhulika, "Nickel-Cobalt Metal-Organic Frameworks Based Flexible Hydrogel as a Wearable Contact Lens for Electrochemical Sensing of Urea in Tear Samples," *Microchimica Acta* 191, no. 5 (2024): 252.

112. Y. N. Reddy, A. De, S. Paul, A. K. Pujari, and J. Bhaumik, "In Situ Nanoarchitectonics of a MOF Hydrogel: A Self-Adhesive and pH-Responsive Smart Platform for Phototherapeutic Delivery," *Biomacromolecules* 24, no. 4 (2023): 1717–1730.

113. Y. Zhu, Z. Chen, C. Wang, et al., "3D Printed Metal Organic Framework Hydrogel for Dye Adsorption and Gas Sensing," *ChemistrySelect* 9, no. 35 (2024): e202402571.

114. S. Pal, Y. Z. Su, Y. W. Chen, C. H. Yu, C. W. Kung, and S. S. Yu, "3D Printing of Metal−Organic Framework-Based Ionogels: Wearable Sensors With Colorimetric and Mechanical Responses," *ACS Applied Materials & Interfaces* 14, no. 24 (2022): 28247–28257.

115. Z. Chen, S. Song, H. Zeng, Z. Ge, B. Liu, and Z. Fan, "3D Printing MOF Nanozyme Hydrogel With Dual Enzymatic Activities and Visualized Glucose Monitoring for Diabetic Wound Healing," *Chemical Engineering Journal* 471 (2023): 144649.

116. A. Nimra, M. Sher, M. Khan, L. A. Shah, J. Fu, and E. A. Ali, "Ex Situ Synergistic Reinforcement of a MOF-Based Supramolecular Polymer Enables Tough, Highly Flexible, and Responsive Artificial Epidermis-Inspired Hydrogels," *Journal of Materials Chemistry C* 13, no. 10 (2025): 5041–5055.

117. S. M. Tawfik, H. Jang, E. A. Ghiaty, et al., "Multifunctional Amphiphilic Nanoporous Zr-MOFs for Detection and Degradation of Nitrophenols, Visual H_2O_2 Sensing, and Antibacterial Applications," *Journal of Hazardous Materials* 495 (2025): 138970.

118. Y. Li, Z. Yu, J. Zhang, et al., "A Metal-Organic Framework Enhanced Single Network Organohydrogel With Superior Low-Temperature Adaptability and UV-Blocking Capability Towards Human-Motion Sensing," *Journal of Materials Chemistry C* 13, no. 2 (2025): 724–734.

119. Q. Xia, W. Li, X. Zou, et al., "Metal-Organic Framework (MOF) Facilitated Highly Stretchable and Fatigue-Resistant Ionogels for Recyclable Sensors," *Materials Horizons* 9, no. 11 (2022): 2881–2892.

120. W. Liu, O. Erol, and D. H. Gracias, "3D Printing of an in Situ Grown MOF Hydrogel With Tunable Mechanical Properties," *ACS Applied Materials & Interfaces* 12, no. 29 (2020): 33267–33275.

121. Y. Wang, Z. Shen, H. Wang, et al., "Progress in Research on Metal Ion Crosslinking Alginate-Based Gels," *Gels* 11, no. 1 (2025): 16.

122. P. Tordi, F. Ridi, P. Samorì, and M. Bonini, "Cation-Alginate Complexes and Their Hydrogels: A Powerful Toolkit for the Development of Next-Generation Sustainable Functional Materials," *Advanced Functional Materials* 35, no. 9 (2025): 2416390.

123. J. Liu, W. Li, J. Li, and J. Li, "Hydrogel-Involved Portable Ratiometric Fluorescence Sensor Based on Eu^{3+}/CDs-Modified Metal-Organic Framework for Detection of Ofloxacin and Tetracycline," *Sensors and Actuators B: Chemical* 422 (2025): 136573.

124. J. Huang, Y. Ma, X. Jiang, J. Xian, Z. Fu, and H. Ouyang, "Robust Luminescent Pyrene-Based Metal-Organic Framework Hydrogel as a pH-Responsive Fluorescence Emitter for Sensitive Immunoassay of Cardiac Troponin I," *Analytical Chemistry* 96, no. 37 (2024): 15042–15049.

125. J. Cao, D. Li, S. Feng, et al., "Highly Specific and Sensitive SERS Detection of Putrescine Using Au Nanobowls@Cu-MOF Embedded in a Hydrogel Nanoreactor," *Small* 21, no. 9 (2025): 2408030.

126. H. Qin, H. Zheng, X. He, et al., "Functional Metal–Organic Frameworks Derived-Nanozyme Integrated Sodium Alginate Hydrogel Microspheres for Visual Total Antioxidant Capacity Detection in Foods," *Chemical Engineering Journal* 513 (2025): 162756.

127. M. M. El Sayed, "Production of Polymer Hydrogel Composites and Their Applications," *Journal of Polymers and the Environment* 31, no. 7 (2023): 2855–2879.

128. Y. Gao, K. Peng, and S. Mitragotri, "Covalently Crosslinked Hydrogels via Step-Growth Reactions: Crosslinking Chemistries, Polymers, and Clinical Impact," *Advanced Materials* 33, no. 25 (2021): 2006362.

129. H. Gao, Y. Han, M. Huang, et al., "Design of Highly Stretchable, Self-Adhesive Ionic Conductive Hydrogels for Wearable Strain Sensors," *Advanced Sensor Research* 4, no. 5 (2025): 2500005.

130. T. Zhang, J. Li, B. Zu, and X. Dou, "Multi-Hydration Induced Zwitterionic Hydrogel With Open Environment Stability for Chemical Sensing," *Advanced Sensor Research* 2, no. 5 (2023): 2200061.

131. M. Singh, J. Zhang, K. Bethel, et al., "Closed-Loop Controlled Photopolymerization of Hydrogels," *ACS Applied Materials & Interfaces* 13, no. 34 (2021): 40365–40378.

132. Y. Hua, H. Xia, L. Jia, et al., "Ultrafast, Tough, and Adhesive Hydrogel Basedon Hybrid Photocrosslinking for Articular Cartilagerepair in Water-Filled Arthroscopy," *Science Advances* 7, no. 35 (2021): eabg0628.

133. H. Liu, H. Peng, Y. Xin, and J. Zhang, "Metal-Organic Frameworks: A Universal Strategy Towards Super-Elastic Hydrogels," *Polymer Chemistry* 10, no. 18 (2019): 2263–2272.

134. M. J. Van Vleet, T. Weng, X. Li, and J. R. Schmidt, "In Situ, Time-Resolved, and Mechanistic Studies of Metal-Organic Framework Nucleation and Growth," *Chemical Reviews* 118, no. 7 (2018): 3681–3721.

135. Y. Chai, Y. Zhang, L. Wang, et al., "In Situ One-Pot Construction of MOF/Hydrogel Composite Beads With Enhanced Wastewater Treatment Performance," *Separation and Purification Technology* 295 (2022): 121225.

136. K. Qin, X. Huang, S. Wang, J. Liang, and Z. Fan, "3D-Printed in Situ Growth of Bilayer MOF Hydrogels for Accelerated Osteochondral Defect Repair," *Advanced Healthcare Materials* 14, no. 2 (2024): 2403840.

137. Y. Tian, L. Zhou, J. Liu, et al., "Metal-Organic Frameworks-Based Moisture Responsive Essential Oil Hydrogel Beads for Fresh-Cut Pineapple Preservation," *Food Chemistry* 451 (2024): 139440.

138. M. S. Rahman, M. N. I. Shiblee, K. Ahmed, et al., "Flexible and Conductive 3D Printable Polyvinylidene Fluoride and Poly(*N*,*N*-

Dimethylacrylamide) Based Gel Polymer Electrolytes," *Macromolecular Materials and Engineering* 305, no. 9 (2020): 2000262.

139. Y. Sun, J. Cui, S. Feng, et al., "Projection Stereolithography 3D Printing High-Conductive Hydrogel for Flexible Passive Wireless Sensing," *Advanced Materials* 36, no. 25 (2024): 2400103.

140. M. N. I. Shiblee, K. Ahmed, M. Kawakami, and H. Furukawa, "4D Printing of Shape-Memory Hydrogels for Soft-Robotic Functions," *Advanced Materials Technologies* 4, no. 8 (2019): 1900071.

141. C. Massaroni, V. Saroli, Z. Aloqalaa, D. L. Presti, and E. Schena, "Extrusion-Based Fused Deposition Modeling for Printing Sensors and Electrodes: Materials, Process Parameters, and Applications," *SmartMat* 6, no. 4 (2025): e70027.

142. M. S. Rahman, A. Phani, and S. Kim, "Toward High-Performance Piezoresistive Polymer Derived SiOC Ceramics Through Masked Stereolithography 3D Printing With β-Silicon Carbide Nanopowder Reinforcement," *Macromolecular Rapid Communications* 45, no. 5 (2024): 2300602.

143. M. M. Sabzehmeidani, S. Gafari, S. Jamali, and M. Kazemzad, "Concepts, Fabrication and Applications of MOF Thin Films in Optoelectronics: A Review," *Applied Materials Today* 38 (2024): 102153.

144. I. Shubhangi, I. Nandi, S. K. Rai, and P. Chandra, "MOF-Based Nanocomposites as Transduction Matrices for Optical and Electrochemical Sensing," *Talanta* 266 (2024): 125124.

145. Y. Zheng, F. Z. Sun, X. Han, J. Xu, and X. H. Bu, "Recent Progress in 2D Metal-Organic Frameworks for Optical Applications," *Advanced Optical Materials* 8, no. 13 (2020): 2000110.

146. Y. Shen, A. Tissot, and C. Serre, "Recent Progress on MOF-Based Optical Sensors for VOC Sensing," *Chemical Science* 13, no. 47 (2022): 13978–14007.

147. S. Yang, S. Sarkar, X. Xie, D. Li, and J. Chen, "Application of Optical Hydrogels in Environmental Sensing," *Energy & Environmental Materials* 7, no. 3 (2023): e12646.

148. C. F. Guimarães, R. Ahmed, A. P. Marques, R. L. Reis, and U. Demirci, "Engineering Hydrogel-Based Biomedical Photonics: Design, Fabrication, and Applications," *Advanced Materials* 33, no. 23 (2021): 2006582.

149. A. Mateescu, Y. Wang, J. Dostalek, and U. Jonas, "Thin Hydrogel Films for Optical Biosensor Applications," *Membranes* 2, no. 1 (2012): 40–69.

150. R. Zang, Y. Liu, Y. Wang, et al., "Defect Engineering Zr-MOF-Endowed Activity-Dimension Dual-Sieving Strategy for Anti-Acid Recognition of Real Phosphoryl Fluoride Nerve Agents," *Advanced Functional Materials* 35, no. 27 (2025): 2425082.

151. D. M. Reynolds, "The Principles of Fluorescence." *Aquatic Organic Matter Fluorescence* (Cambridge University Press, 2014), 3–34.

152. P. Mahata, S. K. Mondal, D. K. Singha, and P. Majee, "Luminescent Rare-Earth-Based MOFs as Optical Sensors," *Dalton Transactions* 46, no. 2 (2017): 301–328.

153. Z. Wang, J. Huang, J. Huang, B. Yu, K. Pu, and F. J. Xu, "Chemiluminescence: From Mechanism to Applications in Biological Imaging and Therapy," *Aggregate* 2, no. 6 (2021): e140.

154. Y. Liu, X. Y. Xie, C. Cheng, Z. S. Shao, and H. S. Wang, "Strategies to Fabricate Metal-Organic Framework (MOF)-Based Luminescent Sensing Platforms," *Journal of Materials Chemistry C* 7, no. 35 (2019): 10743–10763.

155. K. Müller-Buschbaum, F. Beuerle, and C. Feldmann, "MOF Based Luminescence Tuning and Chemical/Physical Sensing," *Microporous and Mesoporous Materials* 216 (2015): 171–199.

156. G. L. Yang, X. L. Jiang, H. Xu, and B. Zhao, "Applications of MOFs as Luminescent Sensors for Environmental Pollutants," *Small* 17, no. 22 (2021): 2005327.

157. Z. Gan and J. Wang, "A MOF-Stabilized Enzyme-Based Colorimetric Biosensor Integrated With pH Test Strips for Portable Detection of *D*-Limonene in Agricultural Applications," *Chemical Engineering Journal* 510 (2025): 161719.

158. Z. K. Yao, F. Guo, W. Q. Luo, et al., "Europium-Based Metal-Organic Framework/Poly(Methyl Methacrylate) Nanocomposite as a Selective and Recyclable Sensor for the Detection of Salicylaldehyde," *ACS Applied Nano Materials* 8, no. 11 (2025): 5739–5747.

159. J. Shen, Y. Dai, F. Xia, and X. Zhang, "Role of Divalent Metal Ions in the Function and Application of Hydrogels," *Progress in Polymer Science* 135 (2022): 101622.

160. B. Yan, "Luminescence Response Mode and Chemical Sensing Mechanism for Lanthanide-Functionalized Metal-Organic Framework Hybrids," *Inorganic Chemistry Frontiers* 8, no. 1 (2021): 201–233.

161. W. Hou, W. Mao, D. Yu, et al., "Photo-Crosslinked Hydrogel as a Sensing Platform for Sensitive Detection of Free Bilirubin in Urine Samples," *Sensors and Actuators B: Chemical* 411 (2024): 135663.

162. L. Rozenberga, W. Bloch, T. A. Gillam, et al., "Europium Metal-Organic Framework Polymer Composites With Enhanced Luminescence and Selective Ferric Ion Sensing," *ACS Applied Polymer Materials* 6, no. 6 (2024): 3544–3553.

163. J. Sheng, X. Liu, F. Liu, Q. Xu, A. Zhu, and X. Zhang, "In-Situ Preparation of Lanthanide Luminescent MOF Hydrogel for Aldehyde Detection," *Journal of Rare Earths* 43, no. 11 (2025): 2375–2384.

164. M. Cheng, Y. Cao, L. Chen, et al., "Portable Fluorescence Histamine Sensor for Assessing Freshness Utilizing Hydrogel Embedded With Dual-Ligand Europium Metal-Organic Framework," *ACS Sensors* 10, no. 6 (2025): 4580–4588.

165. X. Li, S. Zhou, Z. Deng, B. Liu, and B. Gao, "Corn-Inspired High-Density Plasmonic Metal-Organic Frameworks Microneedles for Enhanced SERS Detection of Acetaminophen," *Talanta* 278 (2024): 126463.

166. Y. He, R. Zhang, S. Xie, X. Yang, and Y. Liu, "An Intelligent Hydrogel Detection Platform Based on Colorimetric and SERS Techniques for Real-Time and Sensitive Detection of Kanamycin," *Talanta* 294 (2025): 128246.

167. C. Ji, J. Zhang, R. Fan, T. Sun, and Y. Yang, "Tetranuclear Cluster-Based Eu(III)-Metal-Organic Framework: Ratiometric Platform Design and Ultrasensitive Phenylglyoxylic Acid Detection," *ACS Applied Materials & Interfaces* 15, no. 44 (2023): 51796–51805.

168. F. Q. Yang and L. Ge, "Colorimetric Sensors: Methods and Applications," *Sensors* 23, no. 24 (2023): 9887.

169. Y. Wu, J. Feng, G. Hu, E. Zhang, and H. H. Yu, "Colorimetric Sensors for Chemical and Biological Sensing Applications," *Sensors* 23, no. 5 (2023): 2749.

170. Y. Feng, Y. Wang, and Y. Ying, "Structural Design of Metal–Organic Frameworks With Tunable Colorimetric Responses for Visual Sensing Applications," *Coordination Chemistry Reviews* 446 (2021): 214102.

171. B. Sharma, R. R. Frontiera, A.-I. Henry, E. Ringe, and R. P. Van Duyne, "SERS: Materials, Applications, and the Future," *Materials Today* 15, no. 1–2 (2012): 16–25.

172. R. Singh, R. Gupta, D. Bansal, R. Bhateria, and M. Sharma, "A Review on Recent Trends and Future Developments in Electrochemical Sensing," *ACS Omega* 9, no. 7 (2024): 7336–7356.

173. D. Tao, C. Xie, N. Jaffrezic-Renault, and Z. Guo, "Flexible and Wearable Electrochemical Sensors for Health and Safety Monitoring," *Talanta* 291 (2025): 127863.

174. M. Madadelahi, F. O. Romero-Soto, R. Kumar, U. B. Tlaxcala, and M. J. Madou, "Electrochemical Sensors: Types, Applications, and the Novel Impacts of Vibration and Fluid Flow for Microfluidic Integration," *Biosensors & Bioelectronics* 272 (2025): 117099.

175. N. Kajal, V. Singh, R. Gupta, and S. Gautam, "Metal Organic Frameworks for Electrochemical Sensor Applications: A Review," *Environmental Research* 204 Part C (2022): 112320.

176. X. Hao, W. Song, Y. Wang, J. Qin, and Z. Jiang, "Recent Advancements in Electrochemical Sensors Based on MOFs and Their Derivatives," *Small* 21, no. 4 (2025): 2408624.

177. J. M. Gonçalves, P. R. Martins, D. P. Rocha, et al., "Recent Trends and Perspectives in Electrochemical Sensors Based on MOF-Derived Materials," *Journal of Materials Chemistry C* 9, no. 28 (2021): 8718–8745.

178. L. Fu, A. Yu, and G. Lai, "Conductive Hydrogel-Based Electrochemical Sensor: A Soft Platform for Capturing Analyte," *Chemosensors* 9, no. 10 (2021): 282.

179. Dhanjai, A. Sinha, P. K. Kalambate, et al., "Polymer Hydrogel Interfaces in Electrochemical Sensing Strategies: A Review," *TrAC Trends in Analytical Chemistry* 118 (2019): 488–501.

180. L. Huang, Y. Zhou, X. Hu, and Z. Yang, "Emerging Combination of Hydrogel and Electrochemical Biosensors," *Small* 21, no. 5 (2025): 2409711.

181. J. Liu, G. Sun, W. Sun, X. Zha, N. Wang, and Y. Wang, "Portable Electrochemical Sensor for Adrenaline Detection Using CoNi-MOF-Based CS-PAM Hydrogel," *Journal of Colloid and Interface Science* 671 (2024): 423–433.

182. W. Sun, G. Sun, J. Liu, X. Huang, and Y. Wang, "Integration of MOF/COF Core-Shell Composite Material With Wrinkled Supramolecular Hydrogel: A Portable Electrochemical Sensing Platform for Noradrenaline Bitartrate Detection," *Composites, Part B: Engineering* 291 (2025): 112029.

183. Y. Li, J. Feng, T. Yao, H. Han, Z. Ma, and H. Yang, "Novel Dual-Responsive Hydrogel Composed of Polyacrylamide/Fe-MOF/Zinc Finger Peptide for Construction of Electrochemical Sensing Platform," *Analytica Chimica Acta* 1289 (2024): 342201.

184. Y. Chong, L. Ji, W. Sun, and Y. Wang, "Implantation of Nano-MOFs Into Chitosan/Sodium Alginate Hydrogels: Boosting the Electroanalytical Response of Chlorogenic Acid in Food Samples," *RSC Advances* 15, no. 40 (2025): 33592–33600.

185. J. Liu, W. Sun, G. Sun, X. Huang, S. Lu, and Y. Wang, "Portable Electroanalytical Platform Based on Eco-Friendly Biomass-Based Hydrogels With Bimetallic MOF Composites for Trace Acetaminophen Determination," *ACS Biomaterials Science & Engineering* 11, no. 1 (2025): 649–660.

186. P. Singh, G. Mukundan, and S. Badhulika, "Zns/MnO_2 Metal Organic Framework Based Conductive Hydrogel for Highly Selective and Sensitive Detection of Glutathione in Serum Samples," *Microchemical Journal* 197 (2024): 109727.

187. H. Zhang, J. Zhao, R. Xu, et al., "Composite Paper-Based Electrochemical Aptasensor for AFB1 Detection Using Cu-MOF-Based CS-PAM Hydrogel," *Microchemical Journal* 218 (2025): 115605.

188. C. Liang, H. Zhang, Z. Zhang, et al., "Superhydrophilic Hydrogel-Enhanced Conductive MOF-Based Wearable Sweat Sensors With Anti-Lipid Biofouling Capability," *Microchemical Journal* 215 (2025): 114302.

189. L. Huang, Y. Liu, X. Sheng, et al., "Fabrication of a MIP-CuMOFs@SA-CS Electrochemical Sensor Based on CuHCF for the Highly Selective Detection of Chelerythrine," *Microchemical Journal* 209 (2025): 112743.

190. T. S. Vo and K. Kim, "Recent Trends of Functional Composites and Structures for Electromechanical Sensors: A Review," *Advanced Intelligent Systems* 6, no. 5 (2024): 2300730.

191. Q. Hua, J. Sun, H. Liu, et al., "Skin-Inspired Highly Stretchable and Conformable Matrix Networks for Multifunctional Sensing," *Nature Communications* 9, no. 1 (2018): 244.

192. H. Souri, H. Banerjee, A. Jusufi, et al., "Wearable and Stretchable Strain Sensors: Materials, Sensing Mechanisms, and Applications," *Advanced Intelligent Systems* 2, no. 8 (2020): 2000039.

193. M. Amjadi, K. U. Kyung, I. Park, and M. Sitti, "Stretchable, Skin-Mountable, and Wearable Strain Sensors and Their Potential Applications: A Review," *Advanced Functional Materials* 26, no. 11 (2016): 1678–1698.

194. M. S. Rahman, M. T. Rahman, H. Kumar, K. Kim, and S. Kim, "ZIF-8-Enhanced Multifunctional, High-Performance Nanocomposite Hydrogel-Based Wearable Strain Sensor for Healthcare Applications," *Advanced Composites and Hybrid Materials* 7, no. 5 (2024): 168.

195. M. Khan, T. U. Rahman, L. A. Shah, H. M. Akil, J. Fu, and H. M. Yoo, "Multi-Role Conductive Hydrogels for Flexible Transducers Regulated by MOFs for Monitoring Human Activities and Electronic Skin Functions," *Journal of Materials Chemistry B* 12, no. 25 (2024): 6190–6202.

196. J. Yue, C. Li, X. Ji, et al., "Highly Tough and Conductive Hydrogel Based on Defect-Patched Reduction Graphene Oxide for High-Performance Self-Powered Flexible Sensing Micro-System," *Chemical Engineering Journal* 466 (2023): 143358.

197. Y. L. Ji, Y. Zhang, J. Lu, et al., "Multifunctional Hydrogel Electronics for Synergistic Therapy and Visual Monitoring in Wound Healing," *Advanced Healthcare Materials* 14, no. 9 (2025): 2404723.

198. M. S. Rahman, K. Dixit, M. T. Rahman, K. Kim, and S. Kim, "ZIF-67-Incorporated Multifunctional Nanocomposite Organohydrogel for Wearable Pressure and Temperature Sensing Applications," *Chemical Engineering Journal* 510 (2025): 161532.

199. M. T. Rahman, M. S. Rahman, H. Kumar, K. Kim, and S. Kim, "Metal-Organic Framework Reinforced Highly Stretchable and Durable Conductive Hydrogel-Based Triboelectric Nanogenerator for Biomotion Sensing and Wearable Human-Machine Interfaces," *Advanced Functional Materials* 33, no. 48 (2023): 2303471.

200. J. Yue, J. Du, C. Li, et al., "Tuning the d_{xy} Orbital Energy Level in 2D Cobalt-Organic-Framework via In-Plane Conjugated Phthalocyanine for Self-Powered Sensing," *Advanced Functional Materials* 35, no. 22 (2025): 2418474.

201. W. G. Kim, D. W. Kim, I. W. Tcho, J. K. Kim, M. S. Kim, and Y. K. Choi, "Triboelectric Nanogenerator: Structure, Mechanism, and Applications," *ACS Nano* 15, no. 1 (2021): 258–287.

202. S. Niu and Z. L. Wang, "Theoretical Systems of Triboelectric Nanogenerators," *Nano Energy* 14 (2015): 161–192.

203. F. R. Fan, Z. Q. Tian, and Z. L. Wang, "Flexible Triboelectric Generator," *Nano Energy* 1, no. 2 (2012): 328–334.

204. S. M. Sohel Rana, O. Faruk, M. Robiul Islam, T. Yasmin, K. Zaman, and Z. L. Wang, "Recent Advances in Metal-Organic Framework-Based Self-Powered Sensors: A Promising Energy Harvesting Technology," *Coordination Chemistry Reviews* 507 (2024): 215741.

205. G. Khandelwal, N. P. Maria Joseph Raj, and S. J. Kim, "Materials Beyond Conventional Triboelectric Series for Fabrication and Applications of Triboelectric Nanogenerators," *Advanced Energy Materials* 11, no. 33 (2021): 2101170.

206. H. Cheng, Z. Shao, L. Li, W. Liu, Y. Wei, and Q. Xie, "Applications and Advantages of MOFs-Based Triboelectric Nanogenerators for Self-Powered System," *Coordination Chemistry Reviews* 537 (2025): 216708.

207. M. T. Rahman, Y. S. Kim, M. S. Rahman, J. Y. Lim, and S. Kim, "Bimetallic Nanoporous Carbon-Based Direct-Current Triboelectric Nanogenerators for Biomechanical Energy Harvesting and Sensing," *Chemical Engineering Journal* 519 (2025): 164938.

208. Z. Cai, X. Xiao, Y. Wei, and J. Yin, "Stretchable Polymer Hydrogels Based Flexible Triboelectric Nanogenerators for Self-Powered Bioelectronics," *Biomacromolecules* 26, no. 2 (2025): 787–813.

209. B. Zhang, R. Wang, R. Wang, et al., "Recent Advances in Stretchable Hydrogel-Based Triboelectric Nanogenerators for On-Skin Electronics," *Materials Chemistry Frontiers* 8 (2024): 4003–4028.

210. P. Lu, X. Liao, X. Guo, et al., "Gel-Based Triboelectric Nanogenerators for Flexible Sensing: Principles, Properties, and Applications," *Nano-Micro Letters* 16, no. 1 (2024): 206.

211. X. Zhang, L. Chen, L. Fu, et al., "Dual-Functional Metal-Organic Frameworks-Based Hydrogel Micromotor for Uranium Detection and Removal," *Journal of Hazardous Materials* 467 (2024): 133654.